Light Dark Matter Search with NV Centers: Electron Spin, Nuclear Spin, and Comagnetometry

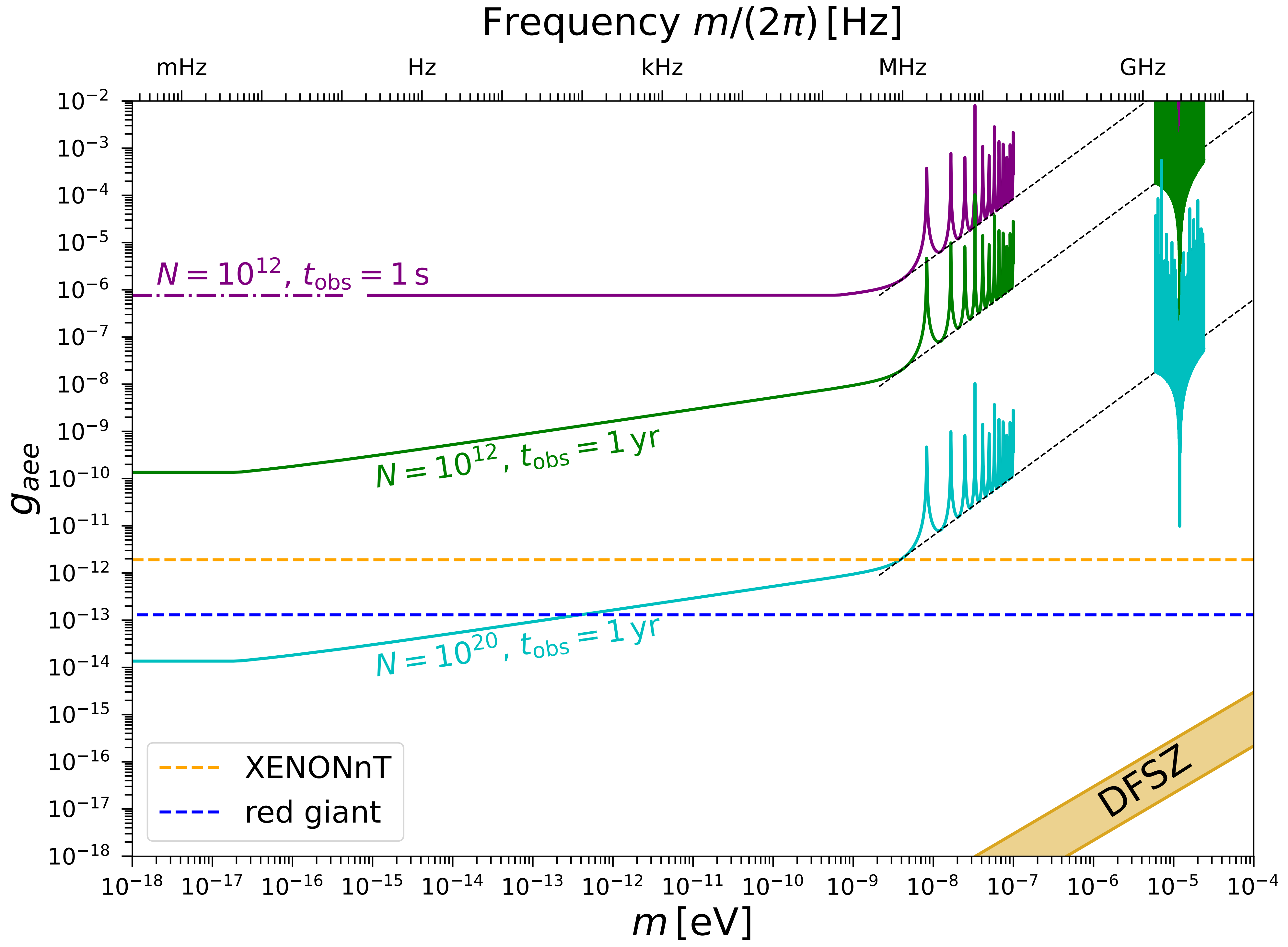

So Chigusa
with M. Hazumi, D. Herbschleb,
Y. Matsuzaki, N. Mizuochi, K. Nakayama
arXiv: 2302.12756 + ongoing works

BERKELEY LAB

International Center for
Quantum-field Measurement Systems for
Studies of the Universe and Particles
WPI research center at KEK

Dark Matter as a hint of new physics

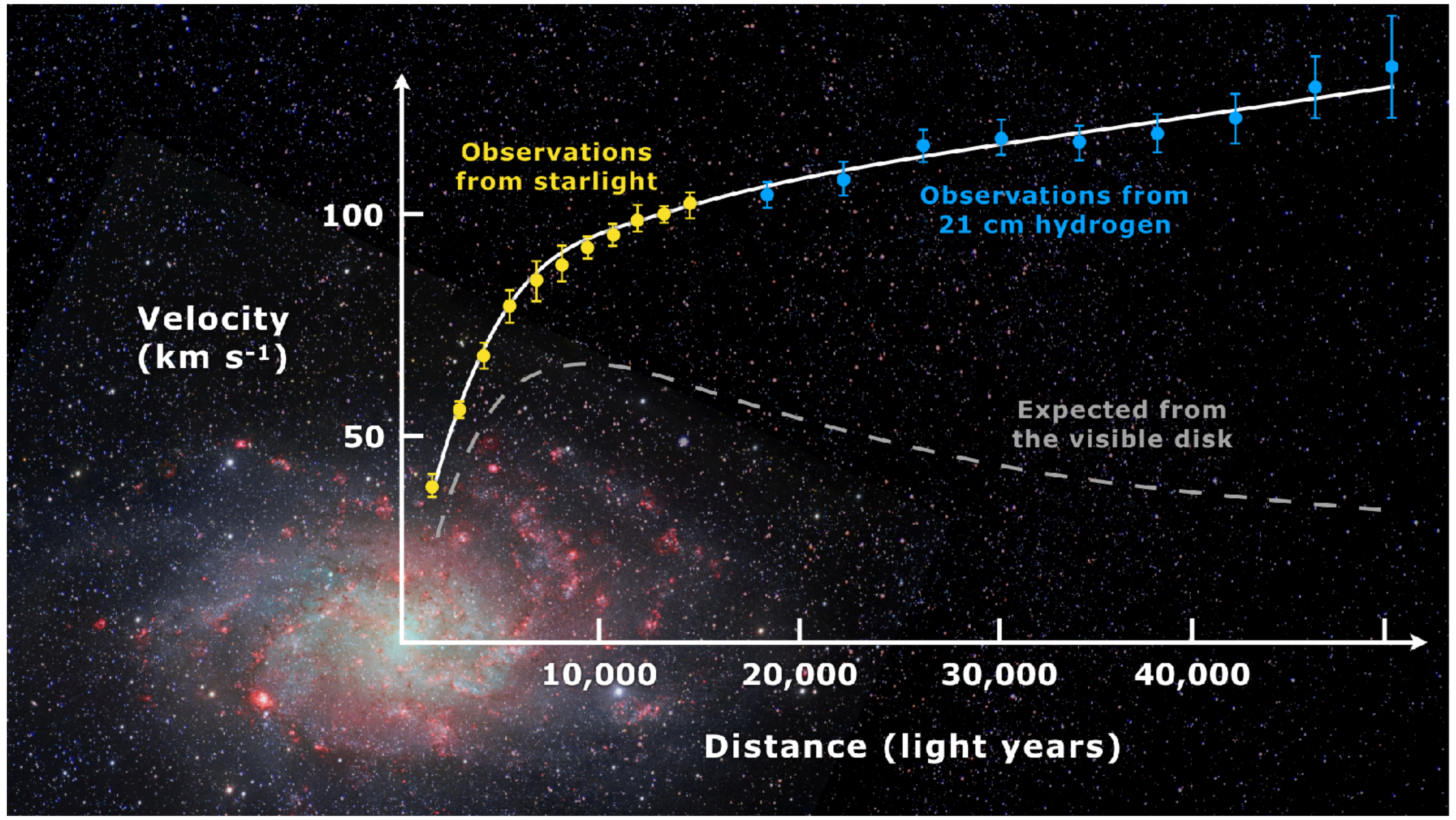

Wikipedia “Galaxy rotation curve”, E. Corbelli, P. Salucci (2000)

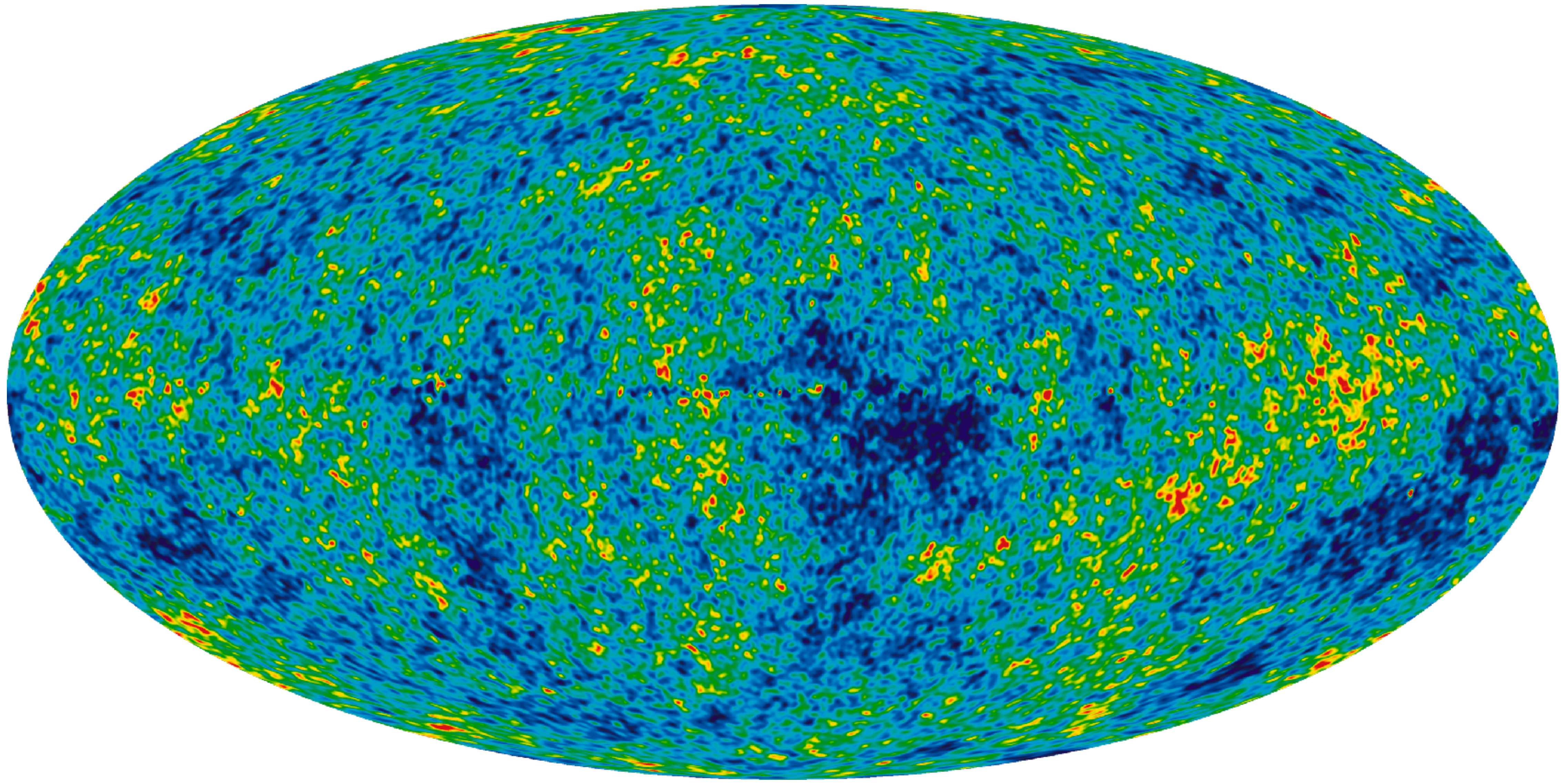

Wikipedia “Cosmic microwave background”, 9 years of WMAP data

“Known”

- ✓ DM existence, abundance
- ✓ Has gravitational interaction

“Unknown”

- ✓ DM mass
- ✓ Non-gravitational interactions

Mass scale of dark matter

(not to scale)

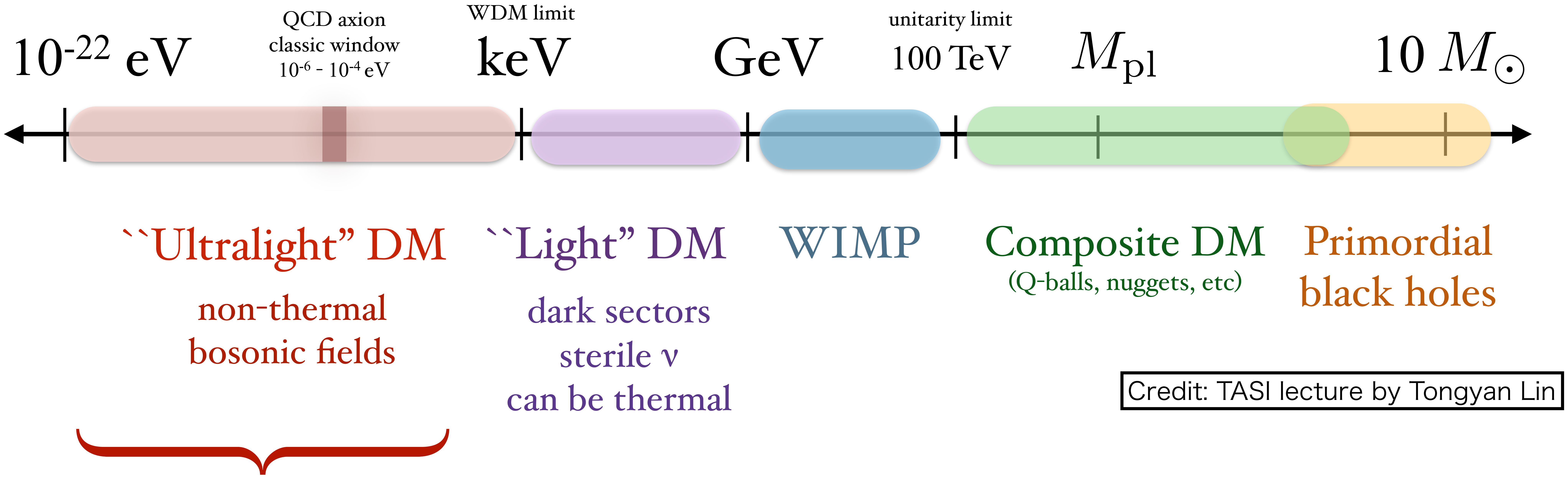

10^{-22} eV

QCD axion
classic window
10^{-6} - 10^{-4} eV

WDM limit
keV

GeV

unitarity limit
100 TeV

$M_{\rm pl}$

10 $M_\odot$

``Ultralight” DM

non-thermal
bosonic fields

``Light” DM

dark sectors
sterile ν
can be thermal

WIMP

Composite DM
(Q-balls, nuggets, etc)

Primordial
black holes

Credit: TASI lecture by Tongyan Lin

$m \ll 30\,\mathrm{eV}$ DM behaves as classical wave

- Classical wave-like dark matter (axion, dark photon) has $O(10^{20})$ mass spread

DM-induced effective magnetic field

- Misalignment mechanism: DM field performs coherent oscillation

$$a(t) \simeq a_0 \cos\left(m_a t - \vec{v}_a \cdot \vec{x} + \delta\right)$$

$$a(t) \simeq a_0 \cos\left(m_a t - \vec{v}'_a \cdot \vec{x} + \delta'\right)$$

with coherence time

$$\tau_a \sim \frac{1}{m_a v_a^2} \sim 7s\left(\frac{10^{-10}\,\mathrm{eV}}{m_a}\right)$$

- DM-SM fermion interactions can be viewed as an effective magnetic field

$$\mathscr{L} = g_{aff}\frac{\partial_\mu a}{2m_f}\bar{f}\gamma^\mu\gamma_5 f \;\rightarrow\; H_{\mathrm{eff}} = \frac{g_{aff}}{m_f}\nabla a \cdot \mathbf{S}_f \;\Rightarrow\; \mathbf{B}_{\mathrm{eff}} \simeq \sqrt{2\rho_{\mathrm{DM}}}\,\frac{g_{aff}}{e}\mathbf{v}_{\mathrm{DM}}\cos(m_a t + \delta) \sim 3\,\mathrm{aT}\left(\frac{g_{aff}}{10^{-10}}\right)$$

- We need a detection method with high sensitivity and broad frequency coverage!

Table of contents

Introduction to NV center

NV center in diamond

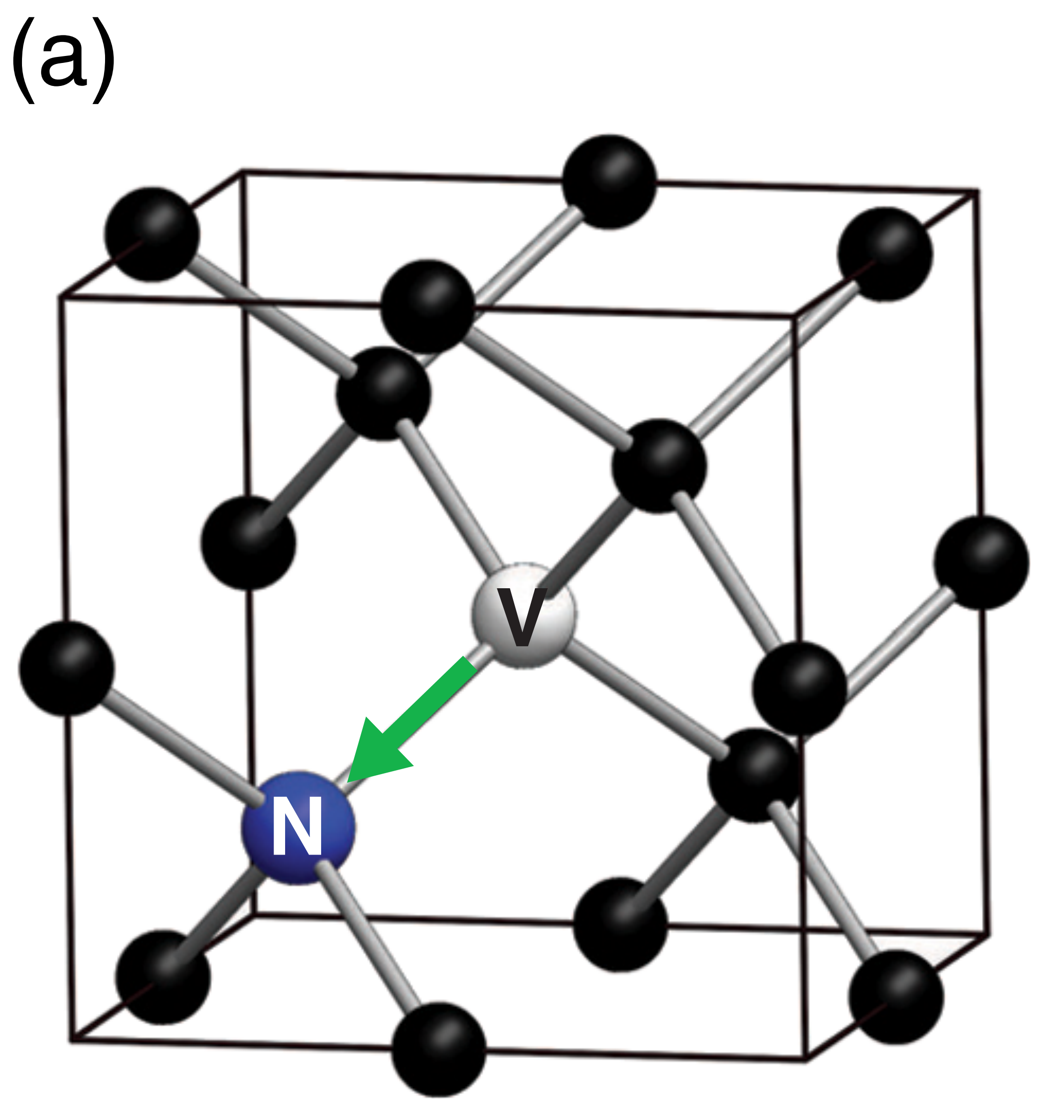

NV ∥ $[1\bar{1}\bar{1}]$

L. M. Pham '13

"pink diamond"

- The stable complex of substitutional nitrogen (N) and vacancy (V) in diamond
- The charged state NV^- has two extra e^-s localized at V
- The ground state: e^- orbital singlet, e^- spin triplet $S = 1$ system

Fluorescence readout

- Fluorescence measurement allows us to read out the e^--spin quantum state

$$|\psi\rangle = \cos\frac{\theta}{2}|0\rangle + \sin\frac{\theta}{2}|\pm\rangle$$

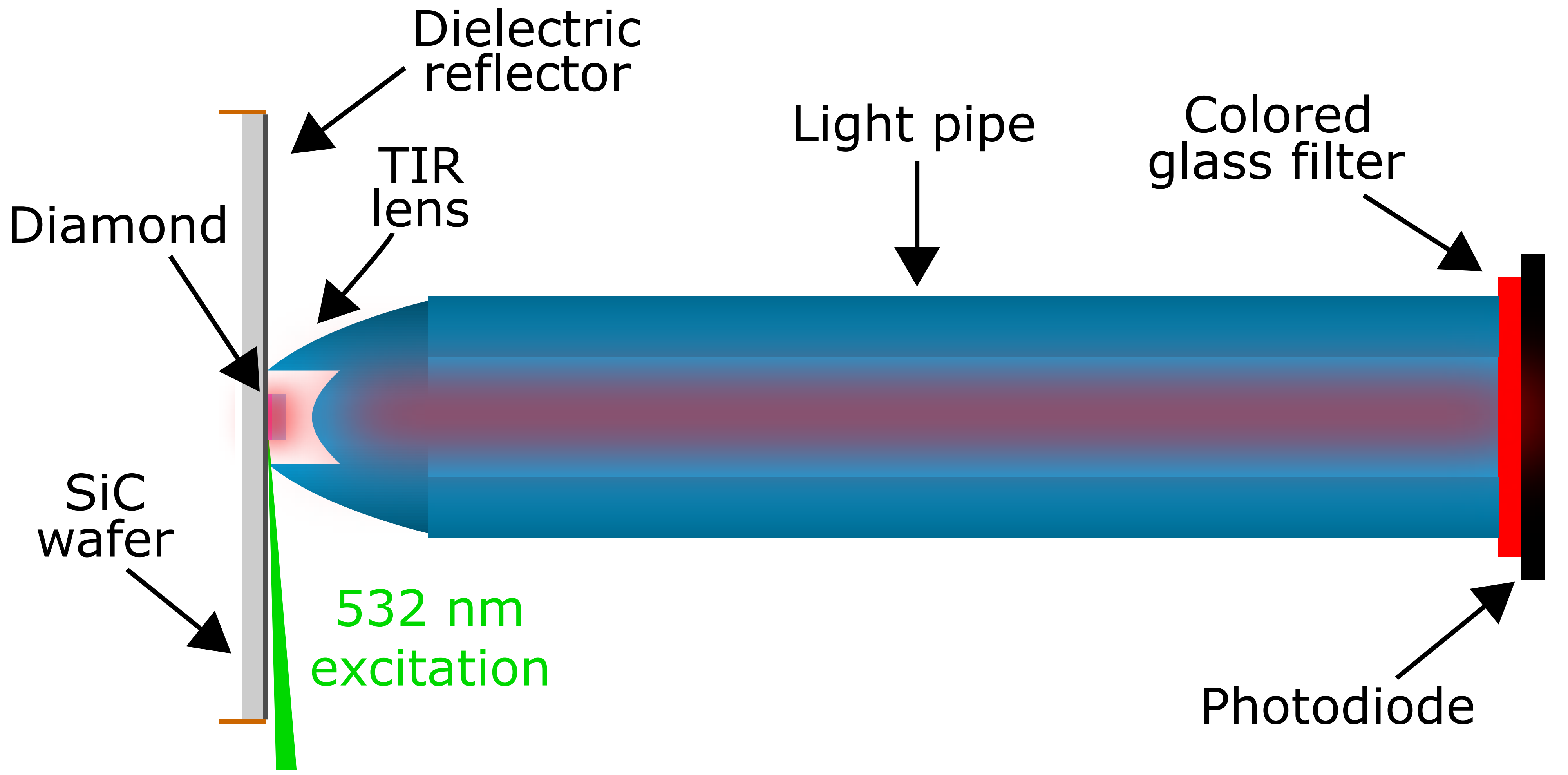

J. F. Barry, et al. ‘23

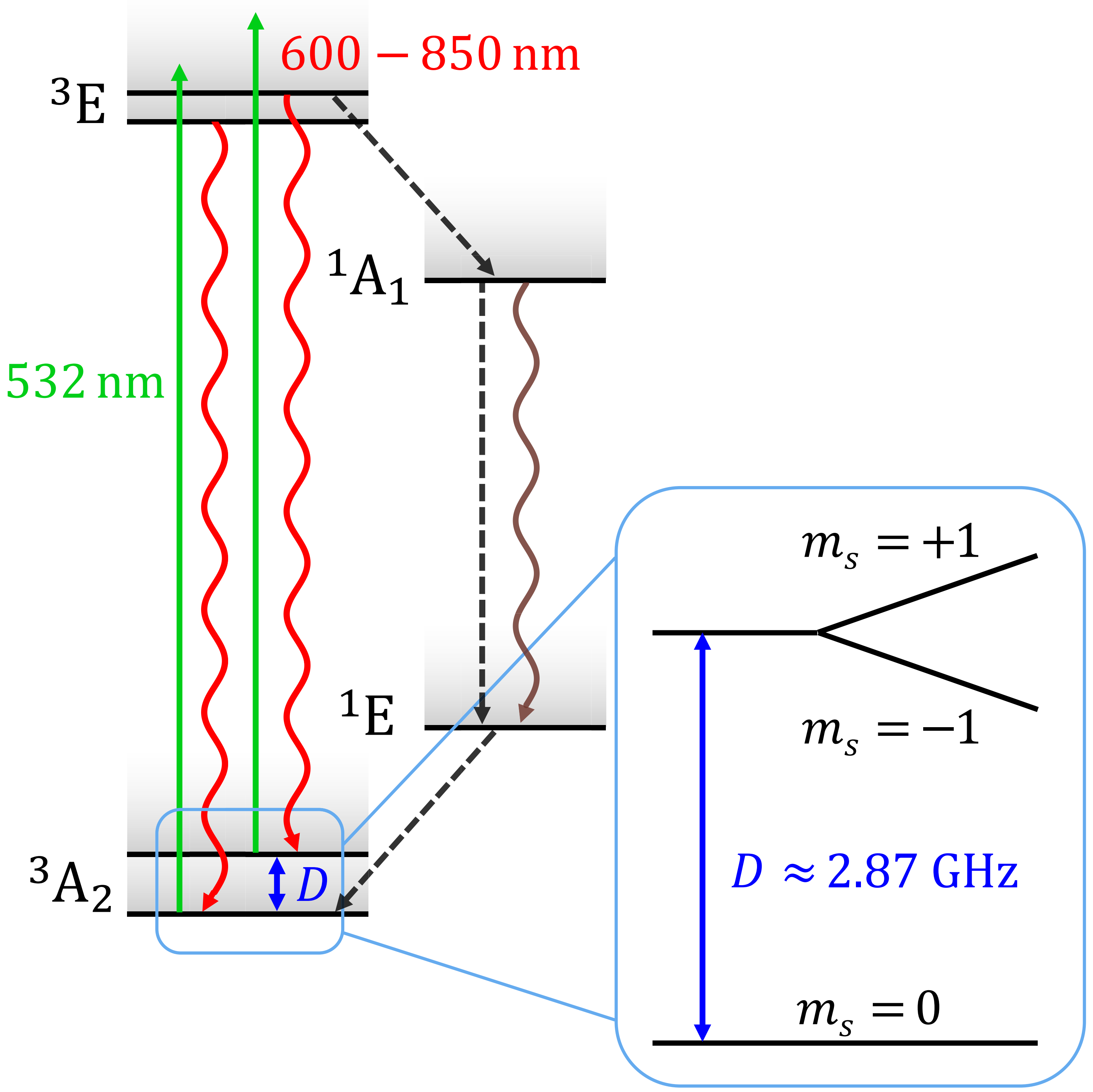

J. M. Schloss, et al. ‘18

NV center as a quantum sensor

- NV center works as a multimodal quantum sensor M. W. Doherty, et al. [1302.3288]
  1. Temperature G. Kucsko, et al. ‘13
  2. Electric field F. Dolde, et al. ‘11
  3. Strain M. Barson, et al. ‘17
  4. Magnetic field (explain later)
     - Sizable relaxation time $\gtrsim 1\,\mu\mathrm{s}$ even at room temperature
     - Wide dynamic range = broad frequency coverage

- Two options
  1. Single NV center (high spacial resolution)
  2. Ensemble of NV centers (high sensitivity)

     $\sim 1-20\,\mathrm{ppm}$ concentration is achieved

T. Wolf, et al. ‘15

DC magnetometry

Rabi cycle

- A transverse driving field $\mathbf{B}_1 = B_{1y}\hat{\mathbf{y}}\sin(2\pi f t)$ with $f = \Delta E \equiv D - \frac{g_e \mu_B}{h} B_z$

  causes transition between $|0\rangle, |-\rangle$

- Time evolution is described by the Rabi cycle

  $$|\psi(t)\rangle = \cos\left(\frac{1}{\sqrt{2}}\gamma_e B_{1y} t\right)|0\rangle + \sin\left(\frac{1}{\sqrt{2}}\gamma_e B_{1y} t\right)|-\rangle$$

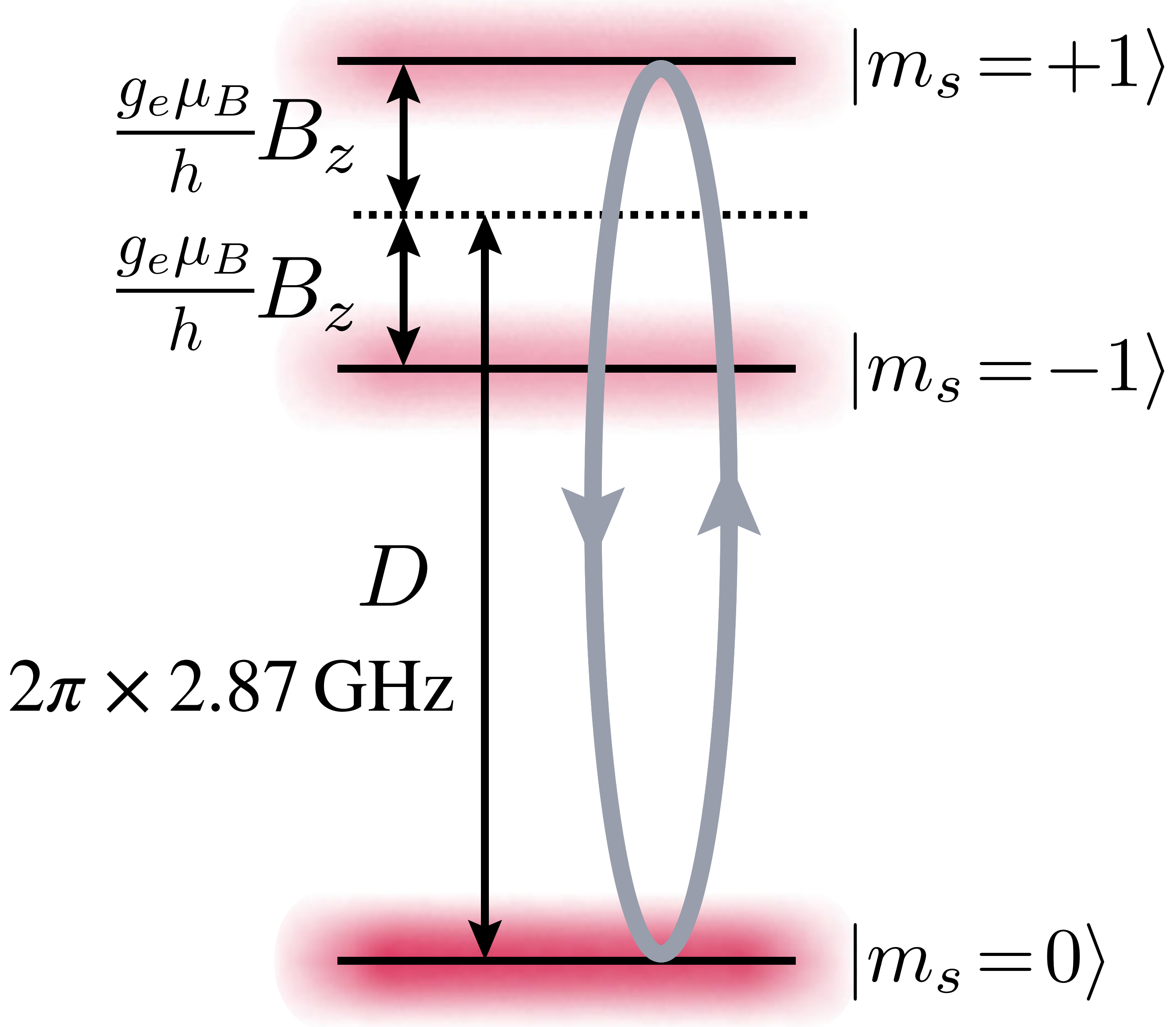

J. F. Barry+ '20

Graphical illustration by Bloch sphere

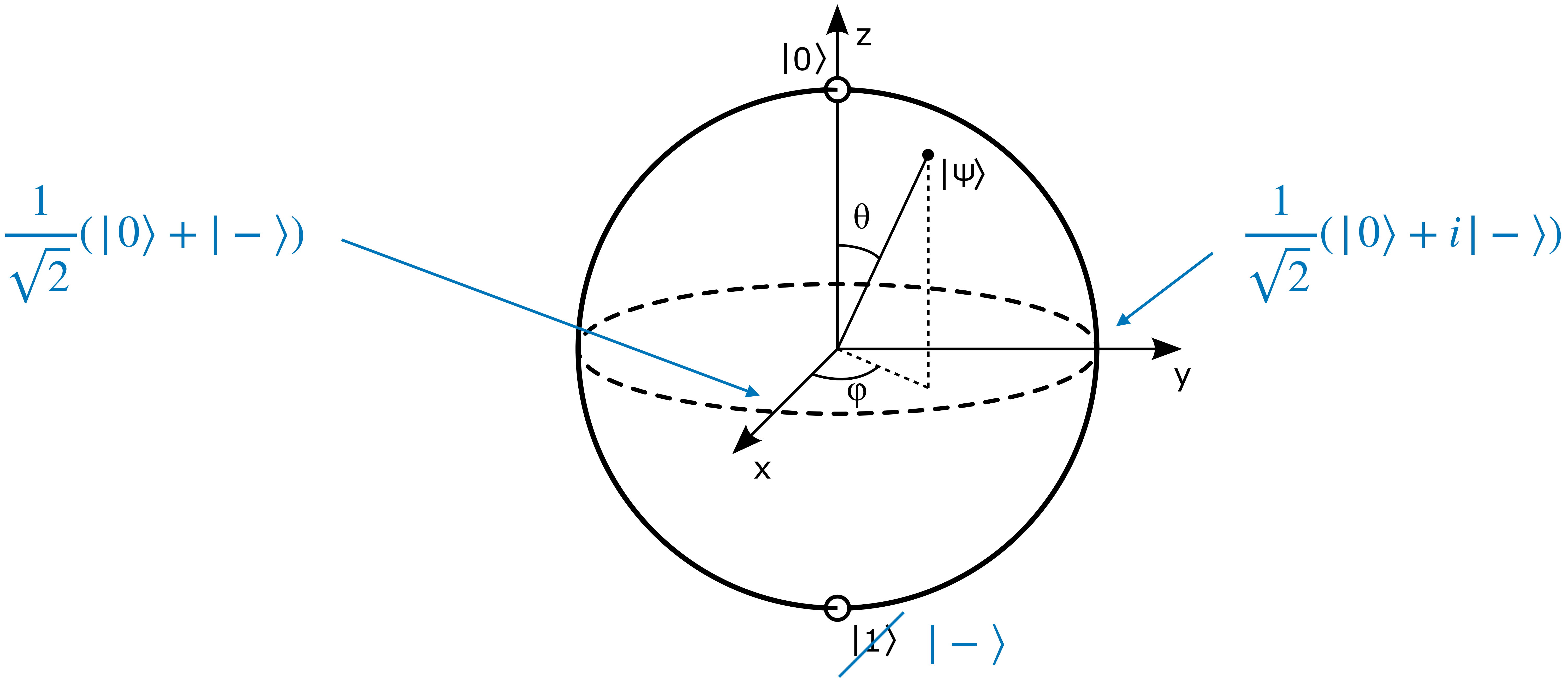

- The qubit system $\{|0\rangle, |-\rangle\}$ is illustrated by the Bloch sphere :

  Map from $|\psi\rangle = \cos\frac{\theta}{2}|0\rangle + \sin\frac{\theta}{2}e^{i\varphi}|-\rangle$ to a sphere S^2

Rabi cycle on Bloch sphere

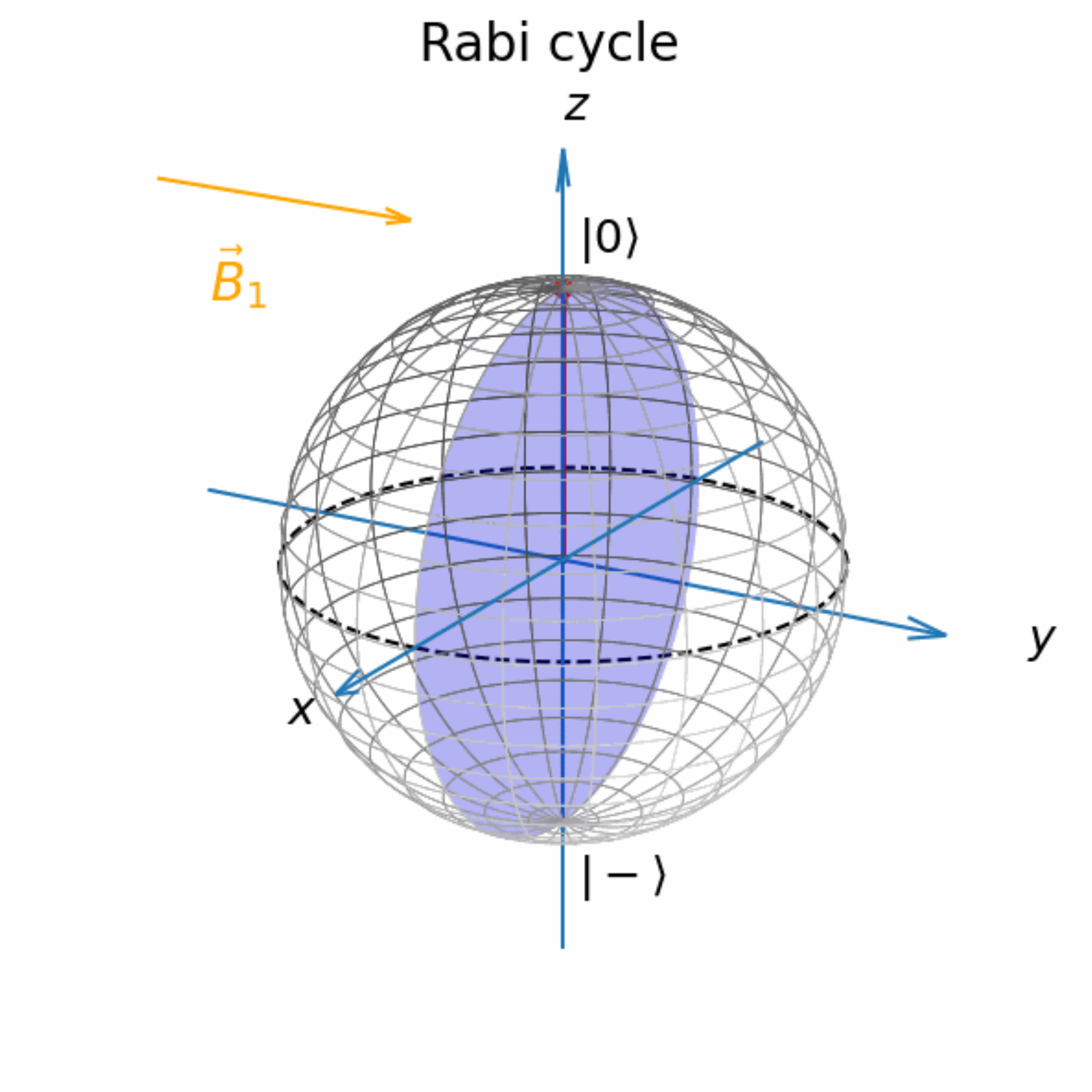

- Rotation around $\vec{B}_1 \propto \hat{\mathbf{y}}$

$$|\psi(t)\rangle = \cos\frac{\theta(t)}{2}|0\rangle + \sin\frac{\theta(t)}{2}|-\rangle, \quad \theta(t) = \sqrt{2}\gamma_e B_{1y}\, t$$

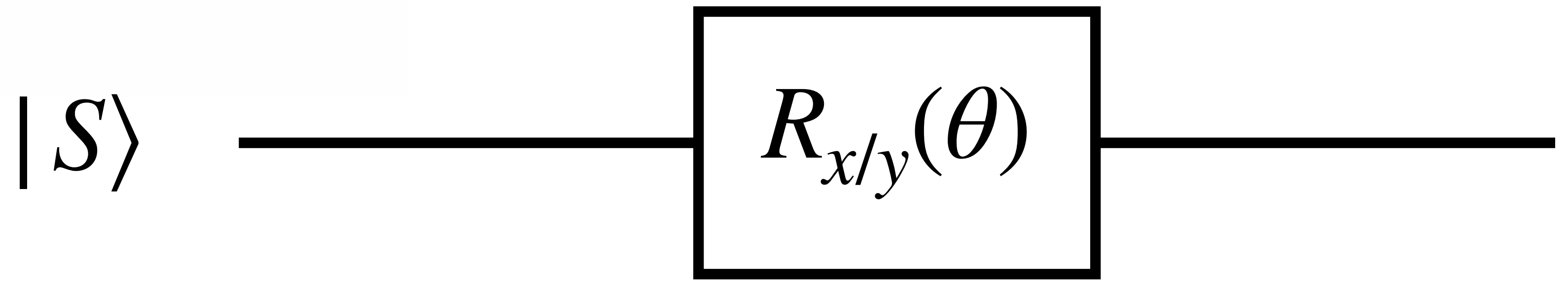

Free precession

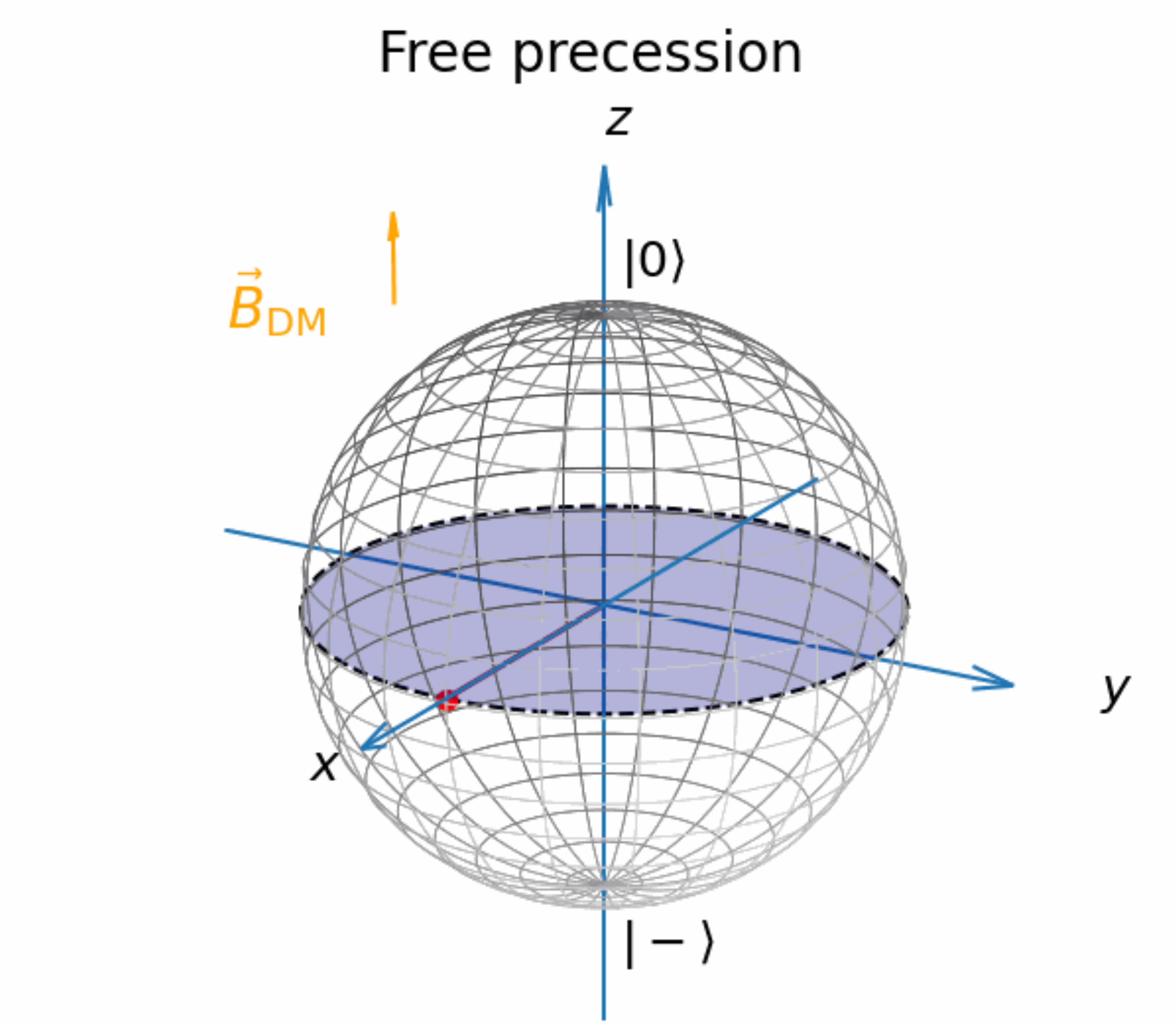

- Weak signal magnetic field $B^z_{\rm DM}$ causes free precession

$$|\psi(\tau)\rangle = \frac{1}{\sqrt{2}}\left(|0\rangle + e^{i\varphi(\tau)}|-\rangle\right) \text{ with } \varphi(\tau) = \gamma_e \int_0^\tau dt\, B^z_{\rm DM}(t) \text{ (} \varphi(\tau) \simeq \gamma_e B^z_{\rm DM}\tau \text{ for DC-like signal)}$$

Ramsey sequence

Ramsey sequence for DC magnetometry

1. $(\pi/2)_y$ pulse
2. Free precession under $\mathbf{B}_{\rm DM}$ for duration τ
3. $(\pi/2)_x$ pulse
4. Fluorescence measurement

- Signal estimate $S \equiv \frac{1}{2}\langle \psi_{\rm fin.} | \sigma_z | \psi_{\rm fin.} \rangle \propto \varphi(\tau) = \gamma_e B^z_{\rm DM}\tau$

  with $\tau \sim T_2^* \sim 1\,\mu{\rm s}$: spin relaxation (dephasing) time

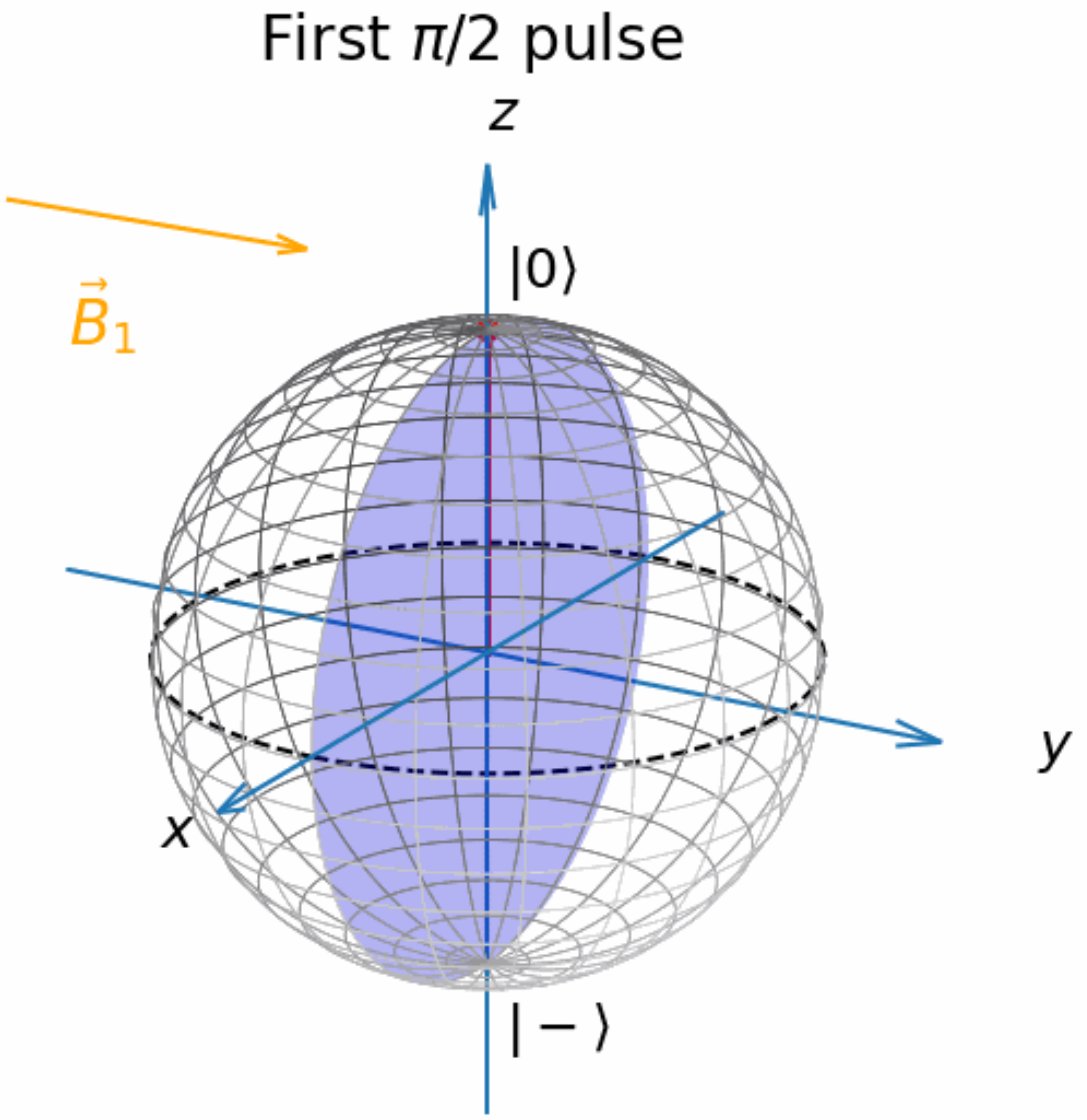

Sensitivity on axion DM

- (Roughly) universal sensitivity to the dc-like region $m \lesssim 2\pi/\tau \sim 10^{-8}\,\mathrm{eV}$

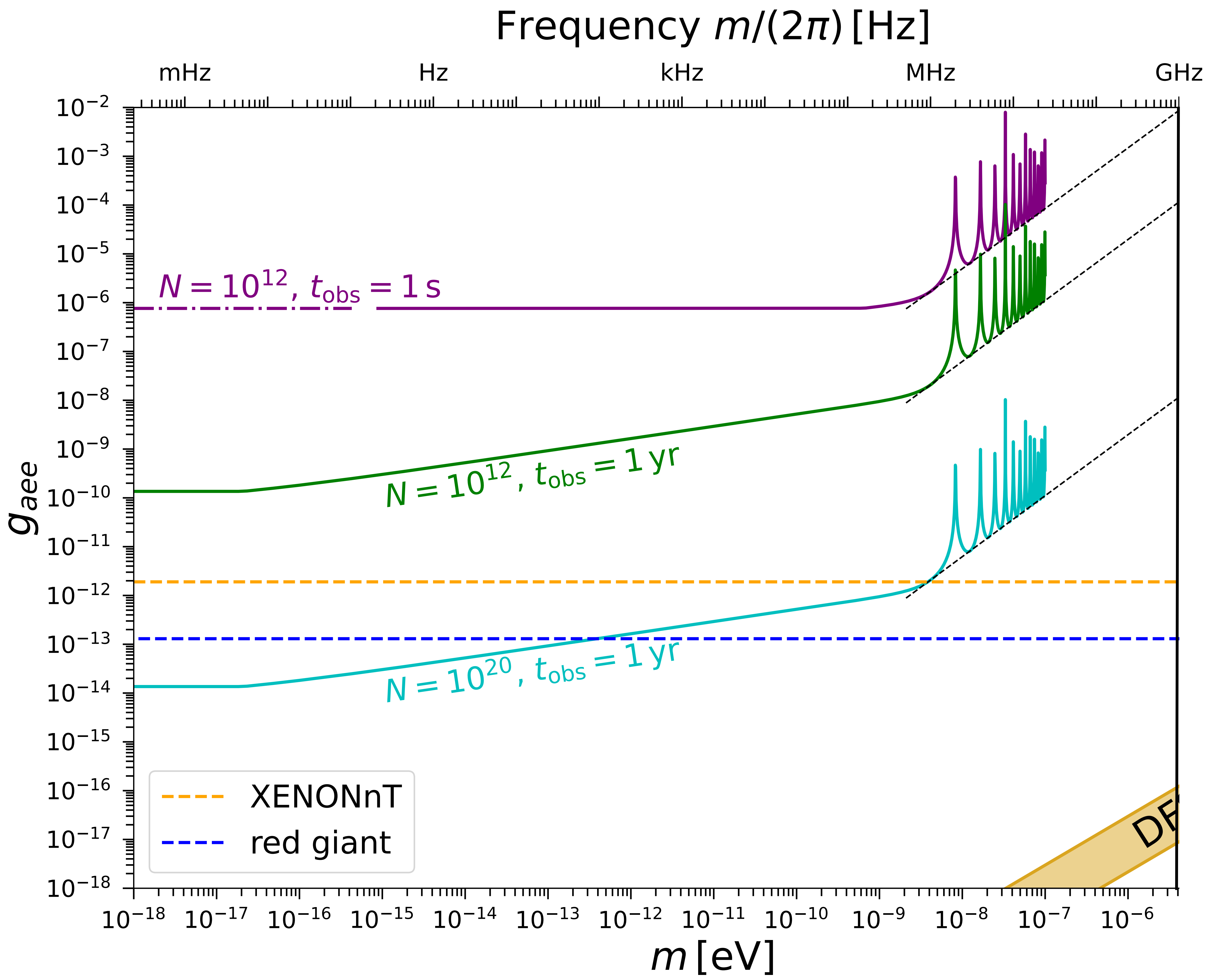

DM on resonance

If $m/2\pi \simeq f$, DM field itself works as a driving field

"Resonance" sequence for $m/2\pi \simeq f$

1. $(\pi/2)_y$ pulse
2. Free precession for duration $\tau \sim T_2^*/2$
3. Fluorescence measurement

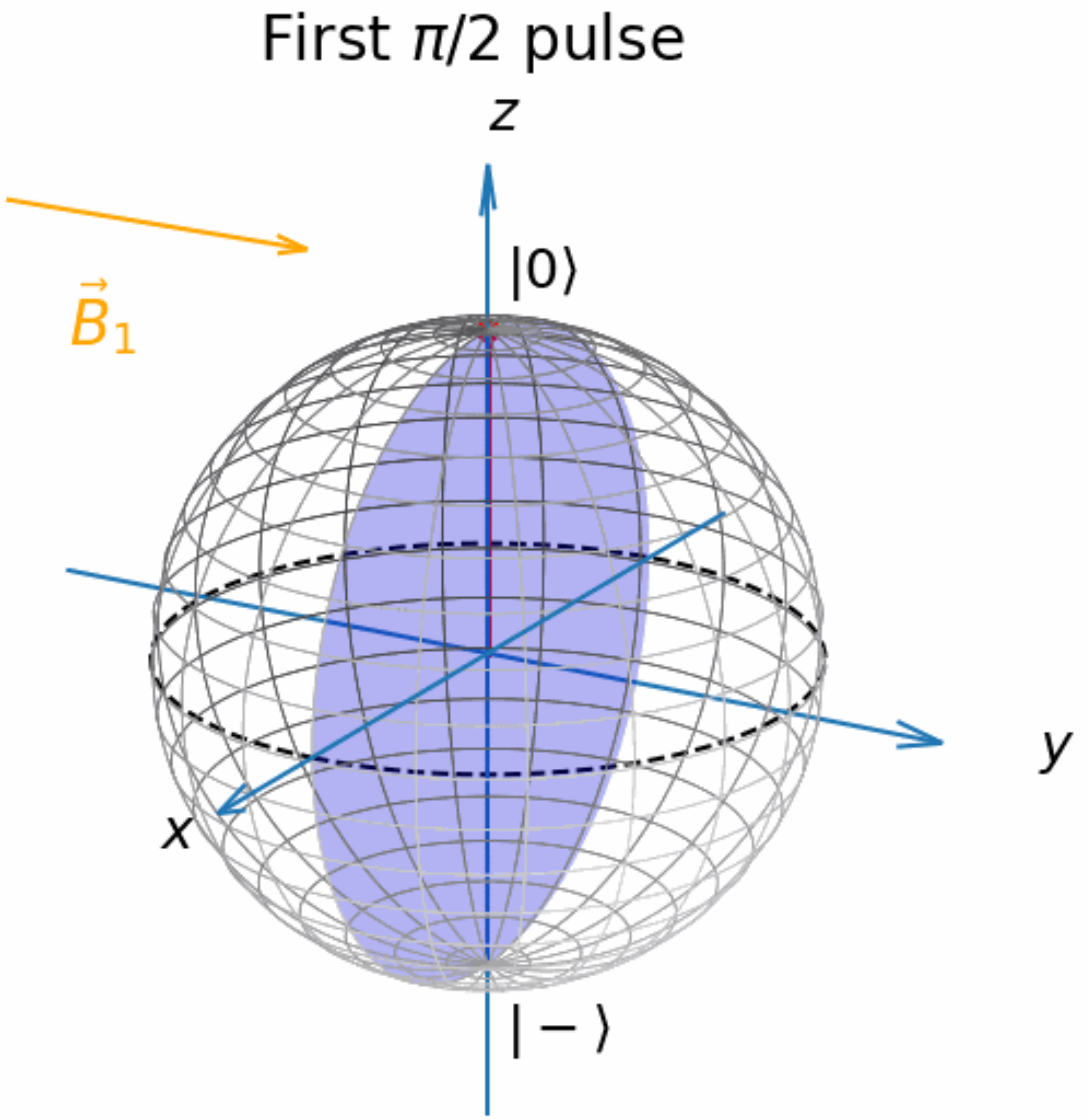

On resonance sensitivity

- Resonance position $m \sim \mathcal{O}(10)\,\mathrm{GHz}$ is tunable with external B_z

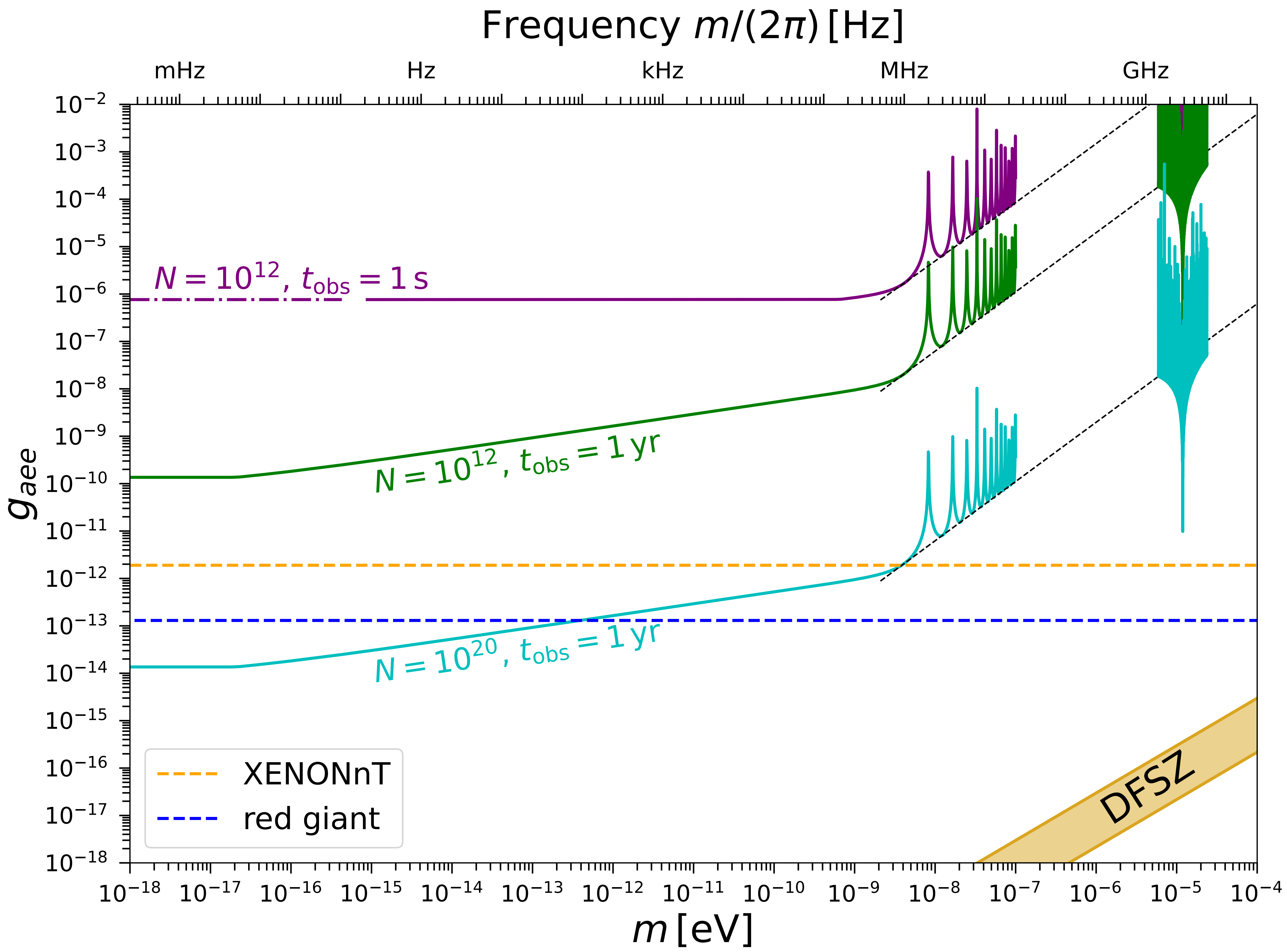

AC magnetometry

Insensitive to fast-oscillating signals

- Fast oscillation leads to cancellation when $m \gtrsim 2\pi/\tau$

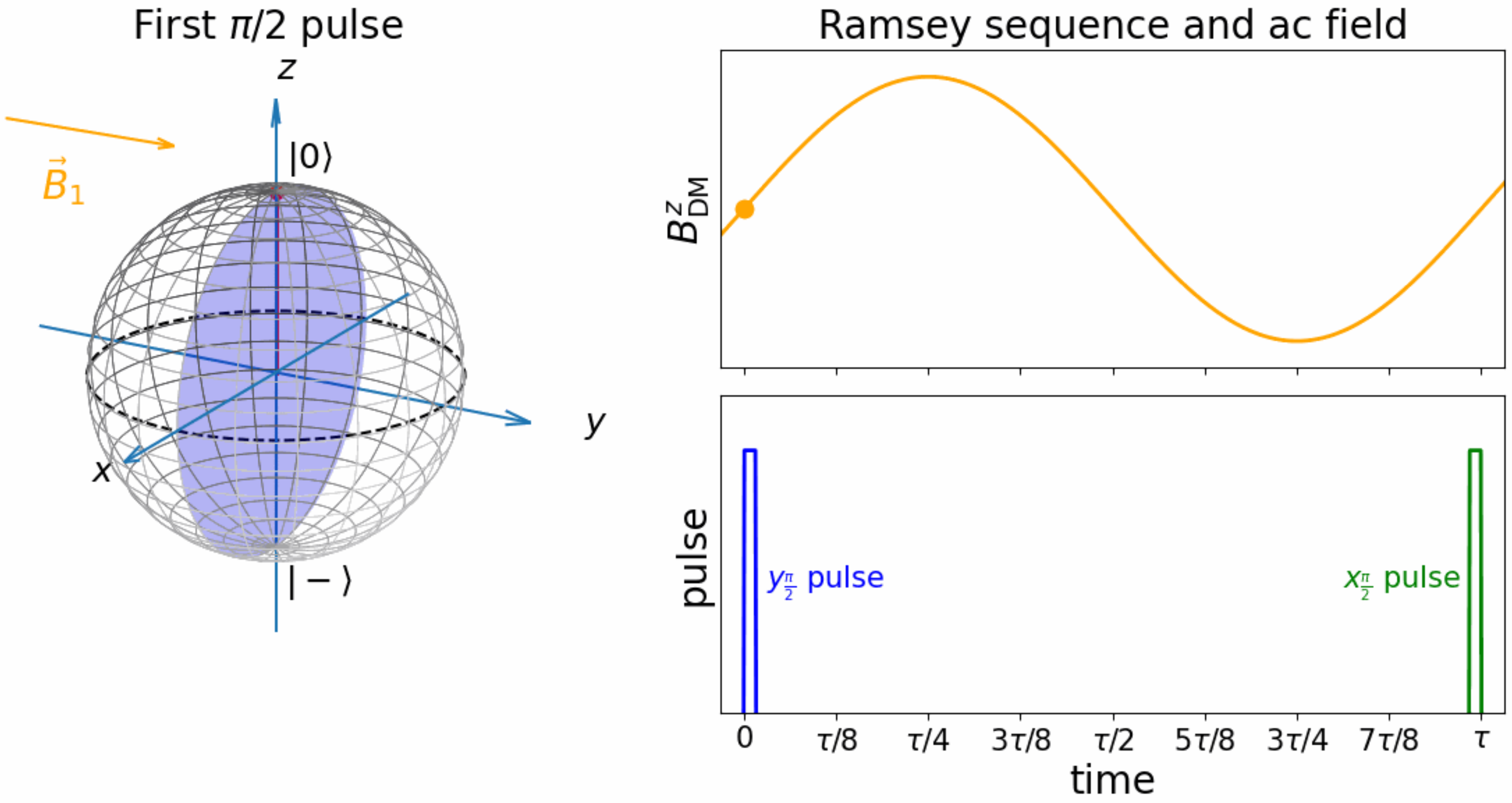

Hahn echo (Dynamic Decoupling)

Hahn echo for ac magnetometry

1. $(\pi/2)_y$ pulse
2. Free precession for $\tau/2$
3. π_y pulse
4. Free precession for $\tau/2$
5. $(\pi/2)_x$ pulse
6. Fluorescence measurement

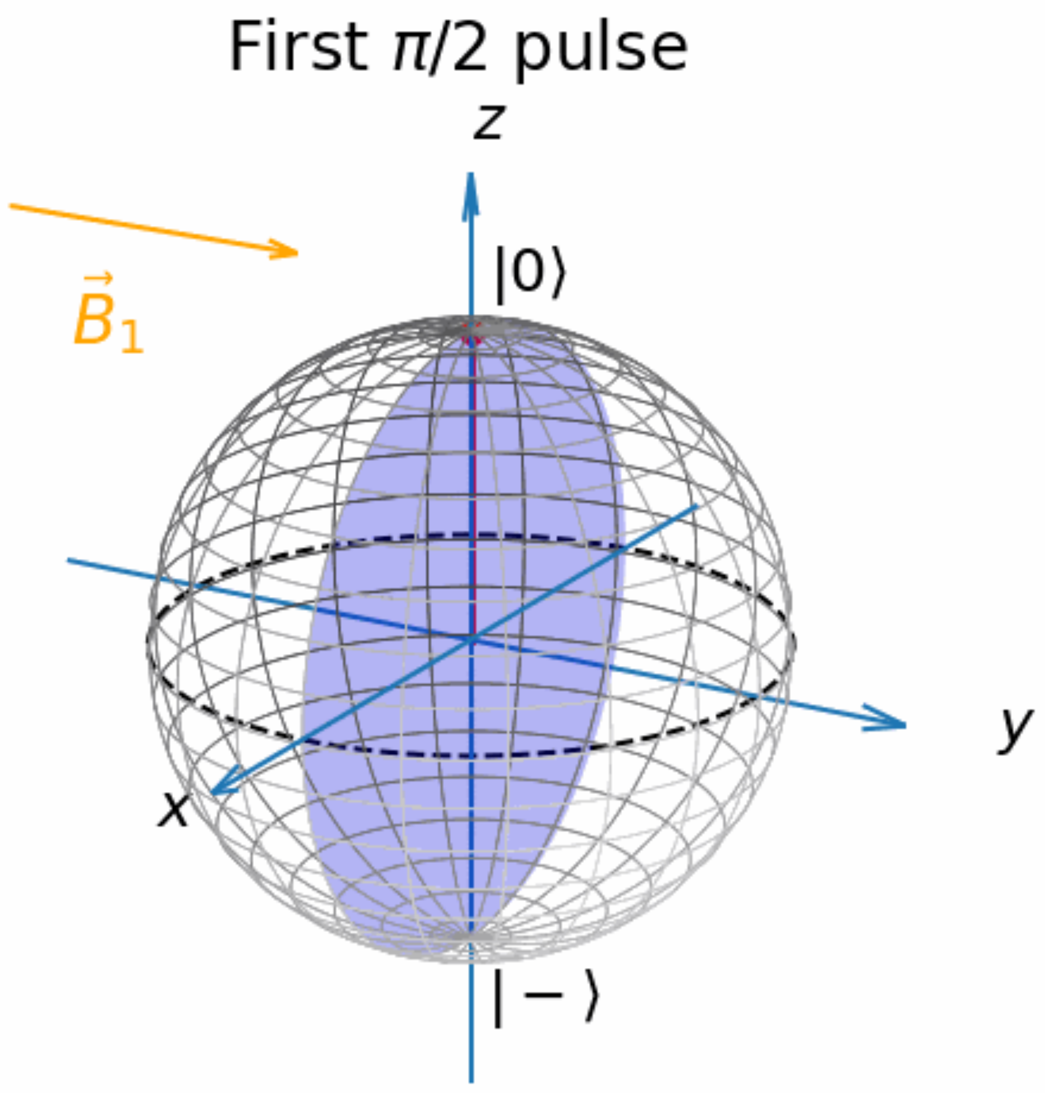

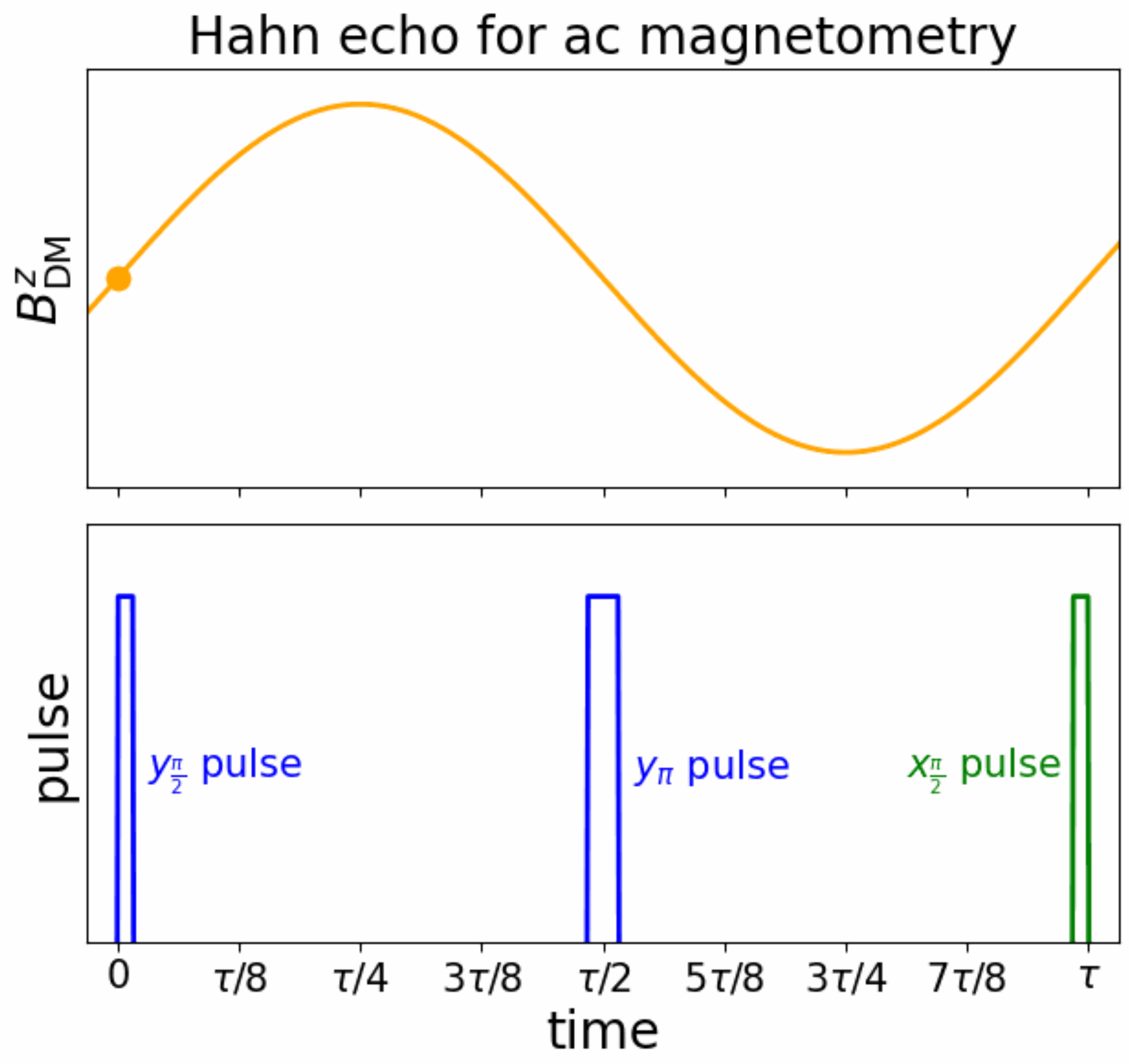

$$\varphi(\tau) = \gamma_e \left(\int_0^{\tau/2} dt\, B^z_{\rm DM}(t) - \int_{\tau/2}^{\tau} dt\, B^z_{\rm DM}(t) \right) \Longrightarrow$$ Targeted at the frequency $\sim 1/\tau$

Longer relaxation time

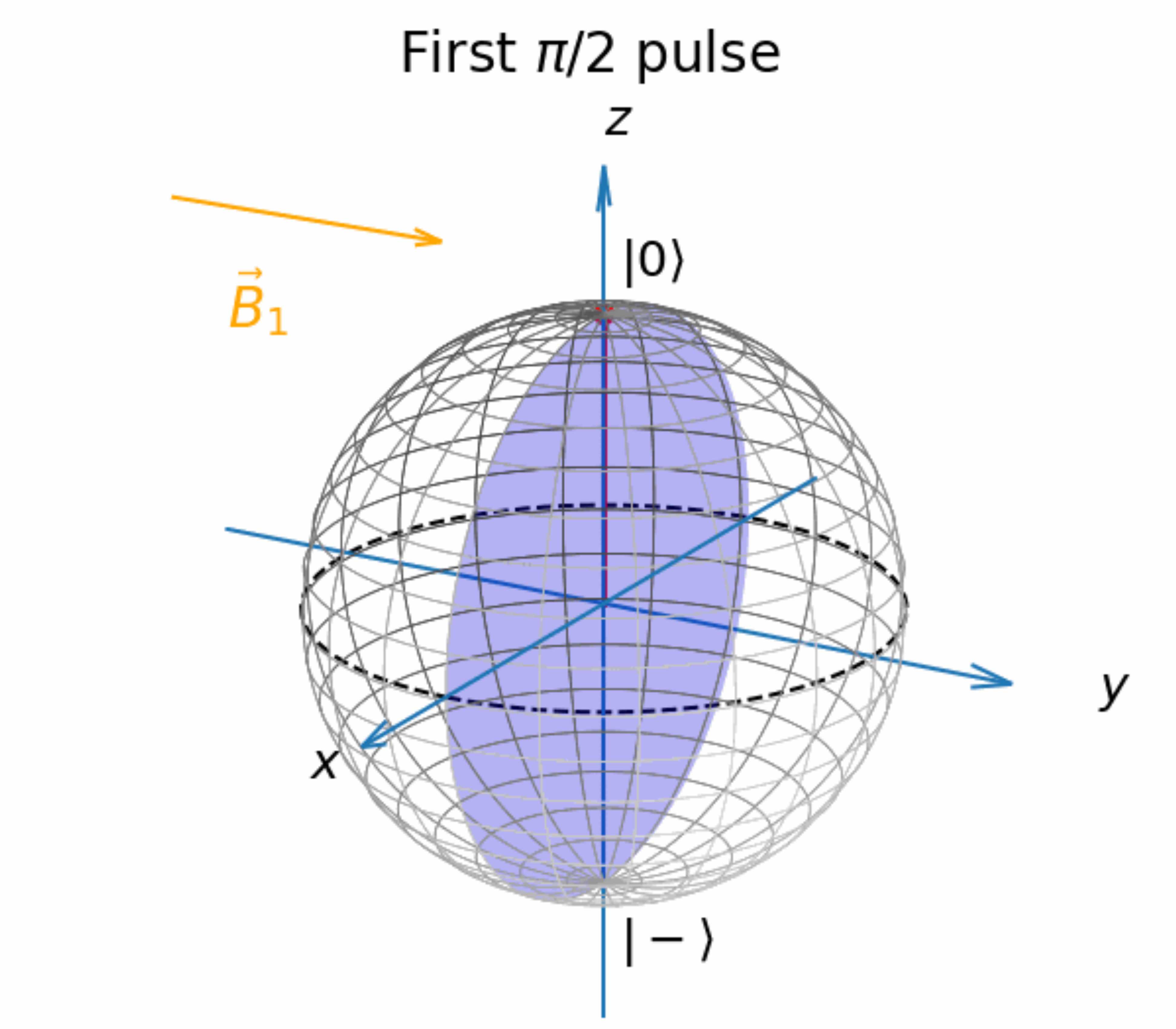

- Any DC effect cancels out from $\varphi(t)$

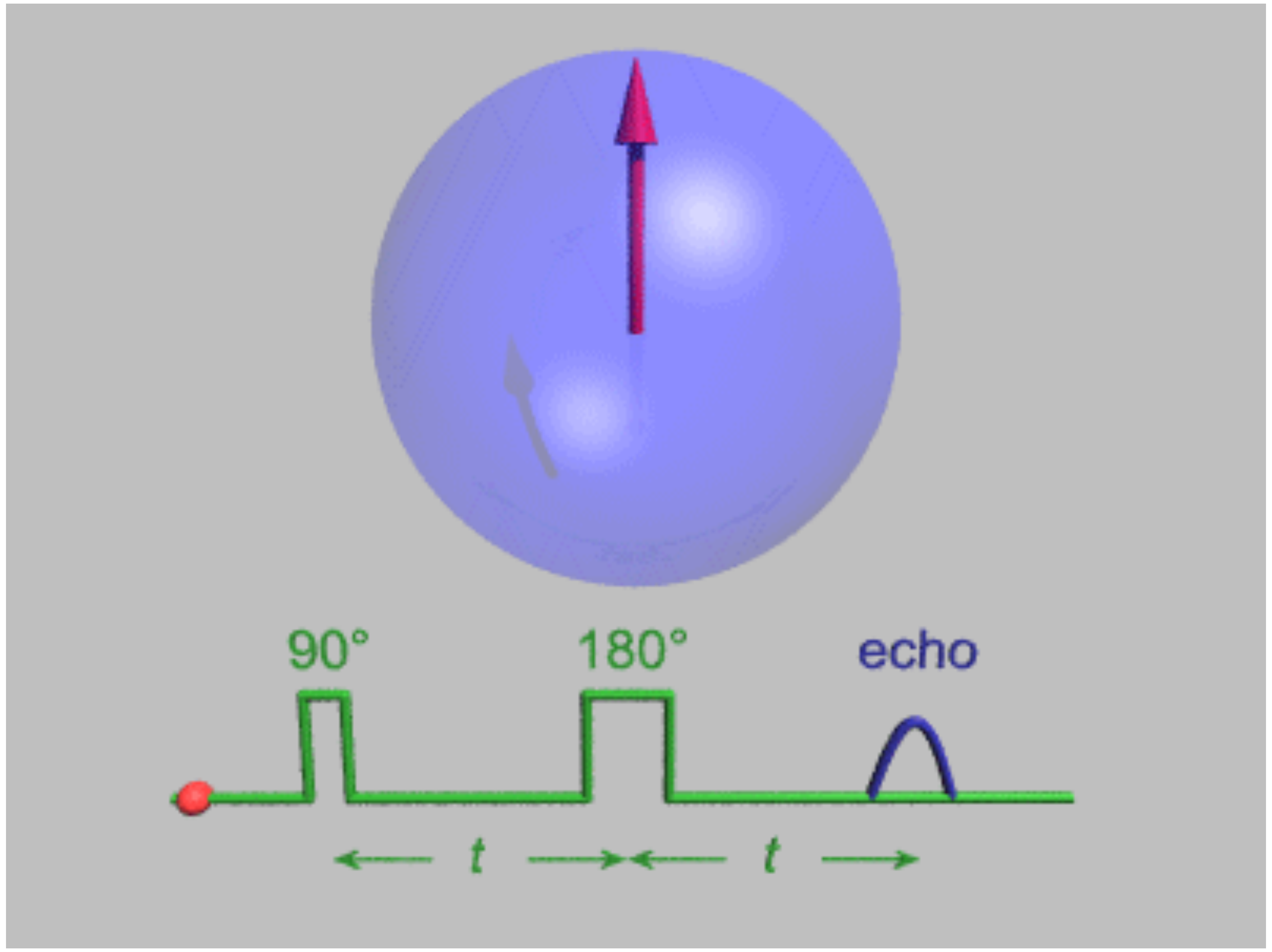

- No dephasing from inhomogeneous DC fields
- Relaxation time $T_2 \sim 100\,\mu\mathrm{s} \gg T_2^* \sim 1\,\mu\mathrm{s}$

Sensitivity on axion DM

- At the target frequency $m \sim 2\pi/T_2 \sim \mathcal{O}(100)\,\mathrm{kHz}$ better sensitivity than Ramsey

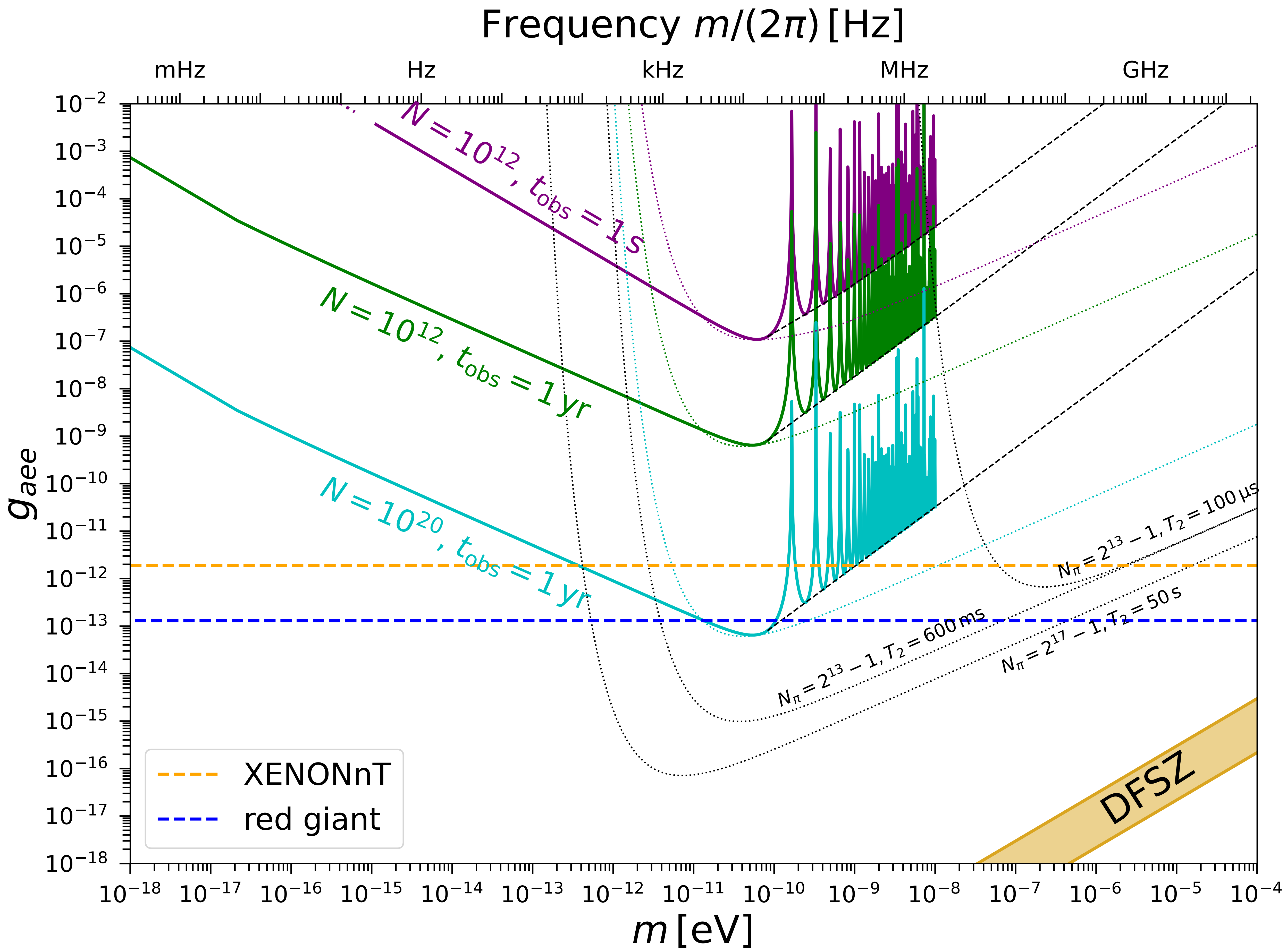

Quantum metrology

- Possible application of involved quantum metrology techniques to NV center

- Example: use of entanglement (the GHZ state)
  - Transmon qubit S. Chen+ [2311.10413]
  - Paul ion trap A. Ito+ [2311.11632]

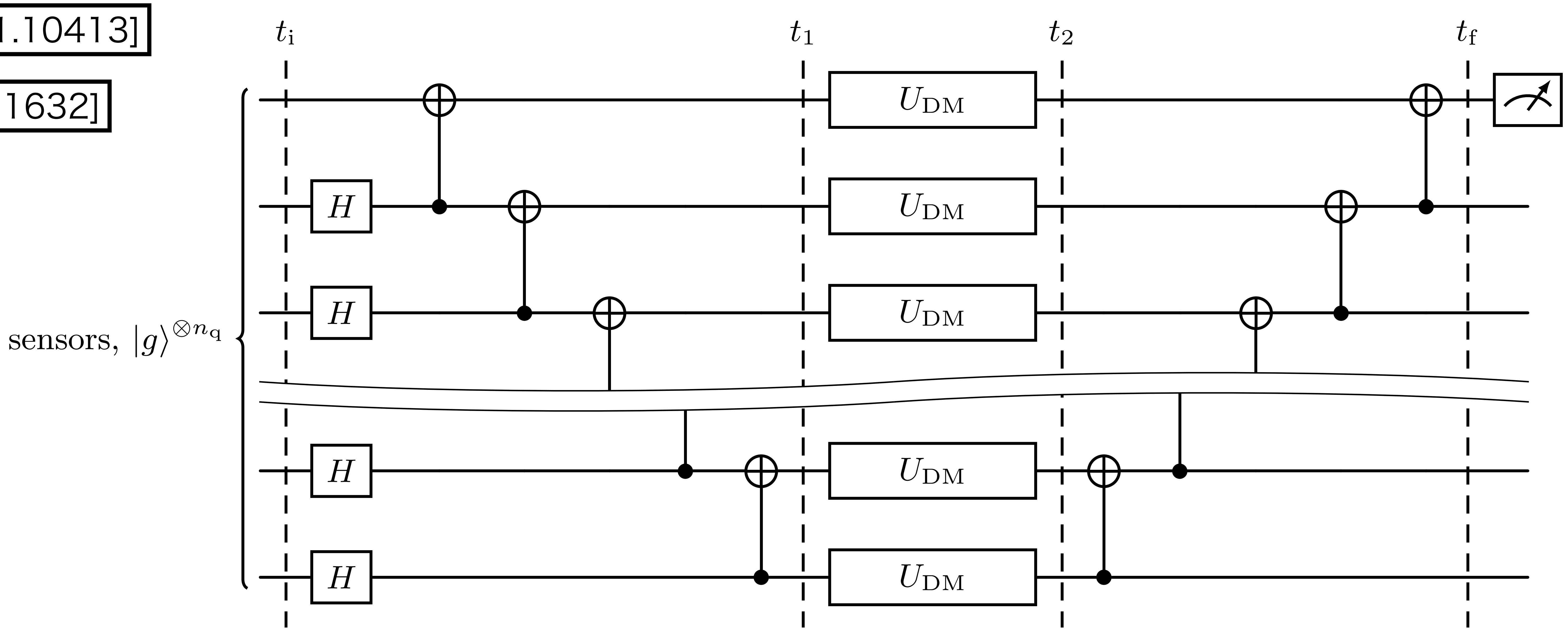

- $|\psi\rangle = \otimes_c \frac{1}{\sqrt{2}}(|0\rangle_c + |1\rangle_c)$

$$\rightarrow \; |\psi\rangle = \frac{1}{\sqrt{2}}\left(|0\rangle^{\otimes N} + |1\rangle^{\otimes N}\right)$$

- $\times N$ gain at the level of amplitude, $\times N^2$ gain of signal

C. L. Degan+ “Quantum sensing” for review

Quantum metrology

- Possible application of involved quantum metrology techniques to NV center

- Example: use of entanglement (the GHZ state)
  - Transmon qubit — S. Chen+ [2311.10413]
  - Paul ion trap — A. Ito+ [2311.11632]

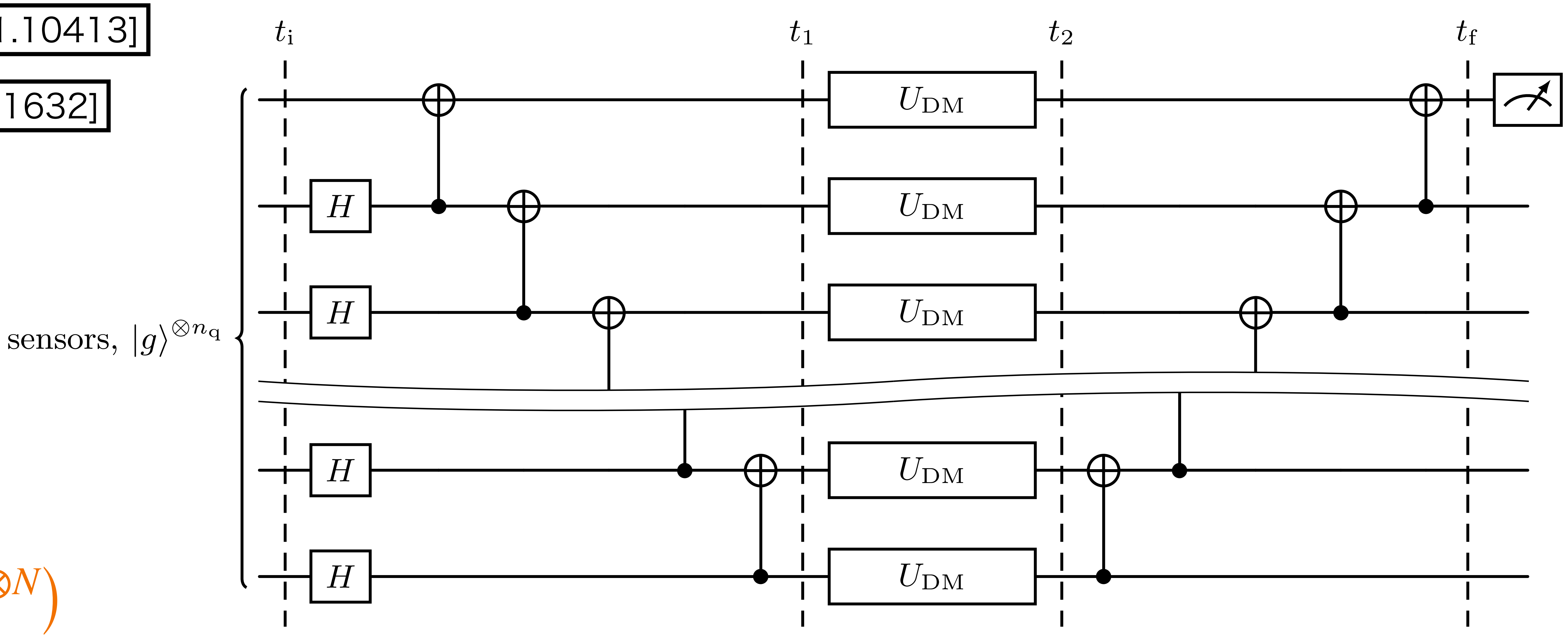

- $$|\psi\rangle = \otimes_c \frac{1}{\sqrt{2}}(|0\rangle_c + e^{i\varphi}|1\rangle_c)$$

$$\rightarrow \; |\psi\rangle = \frac{1}{\sqrt{2}}\left(|0\rangle^{\otimes N} + e^{iN\varphi}|1\rangle^{\otimes N}\right)$$

- $\times N$ gain at the level of amplitude, $\times N^2$ gain of signal

C. L. Degan+ “Quantum sensing” for review

Nuclear spins

Manipulation of nuclear spins

- Mixing between e^- $(\vec{S})$ and $^{14}\mathrm{N}$ $(\vec{I})$ spin states caused by $H_{\mathrm{hyp}} = AS_zI_z$ allows the controlled-manipulation

Dutt+, Science (2007)
Neumann+, Nature (2010)
van der Sar+, Nature (2012)

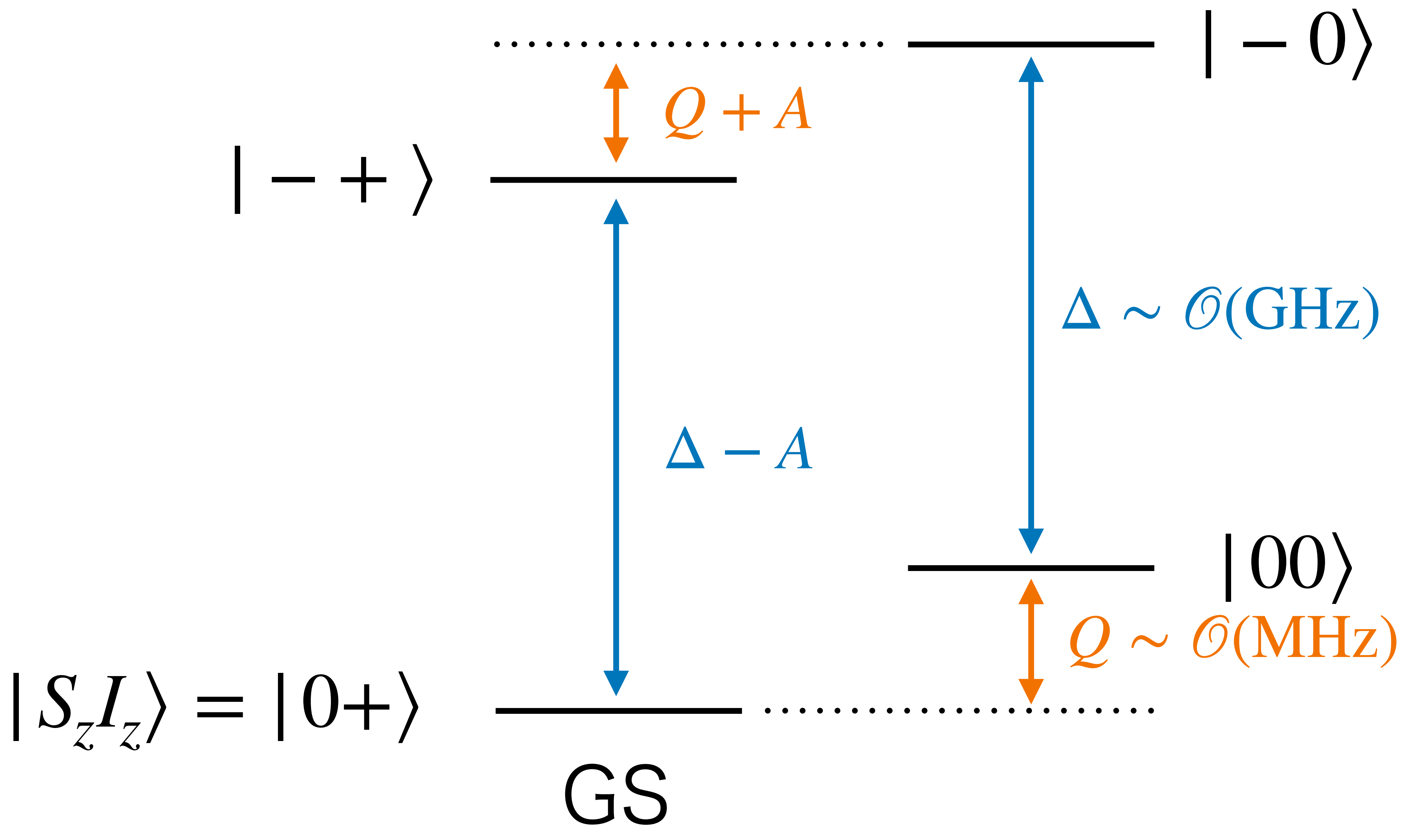

Manipulation of nuclear spins

- Mixing between e^- ($\vec{S}$) and $^{14}\mathrm{N}$ ($\vec{I}$) spin states caused by $H_{\mathrm{hyp}} = AS_zI_z$ allows the controlled-manipulation

Dutt+, Science (2007)
Neumann+, Nature (2010)
van der Sar+, Nature (2012)

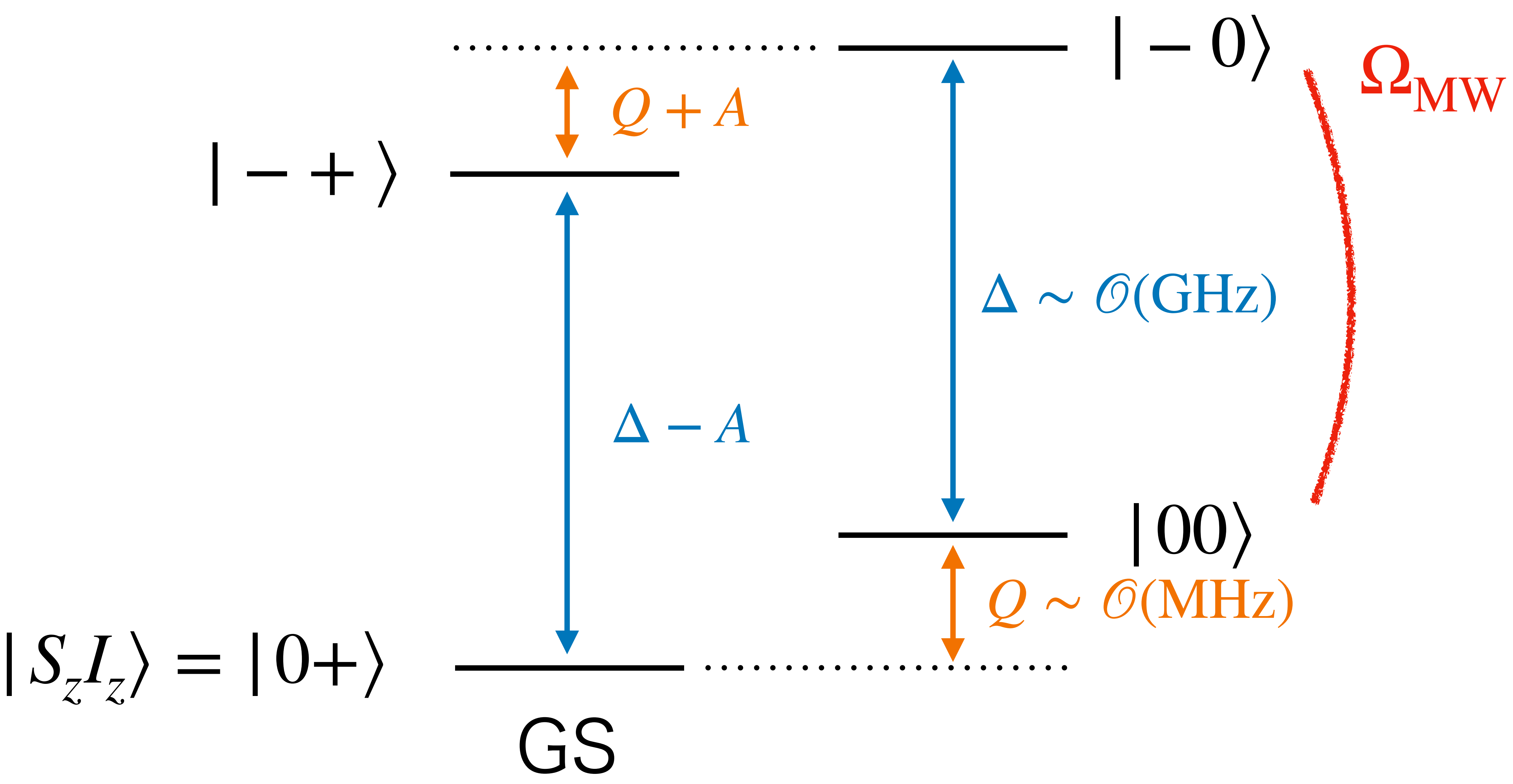

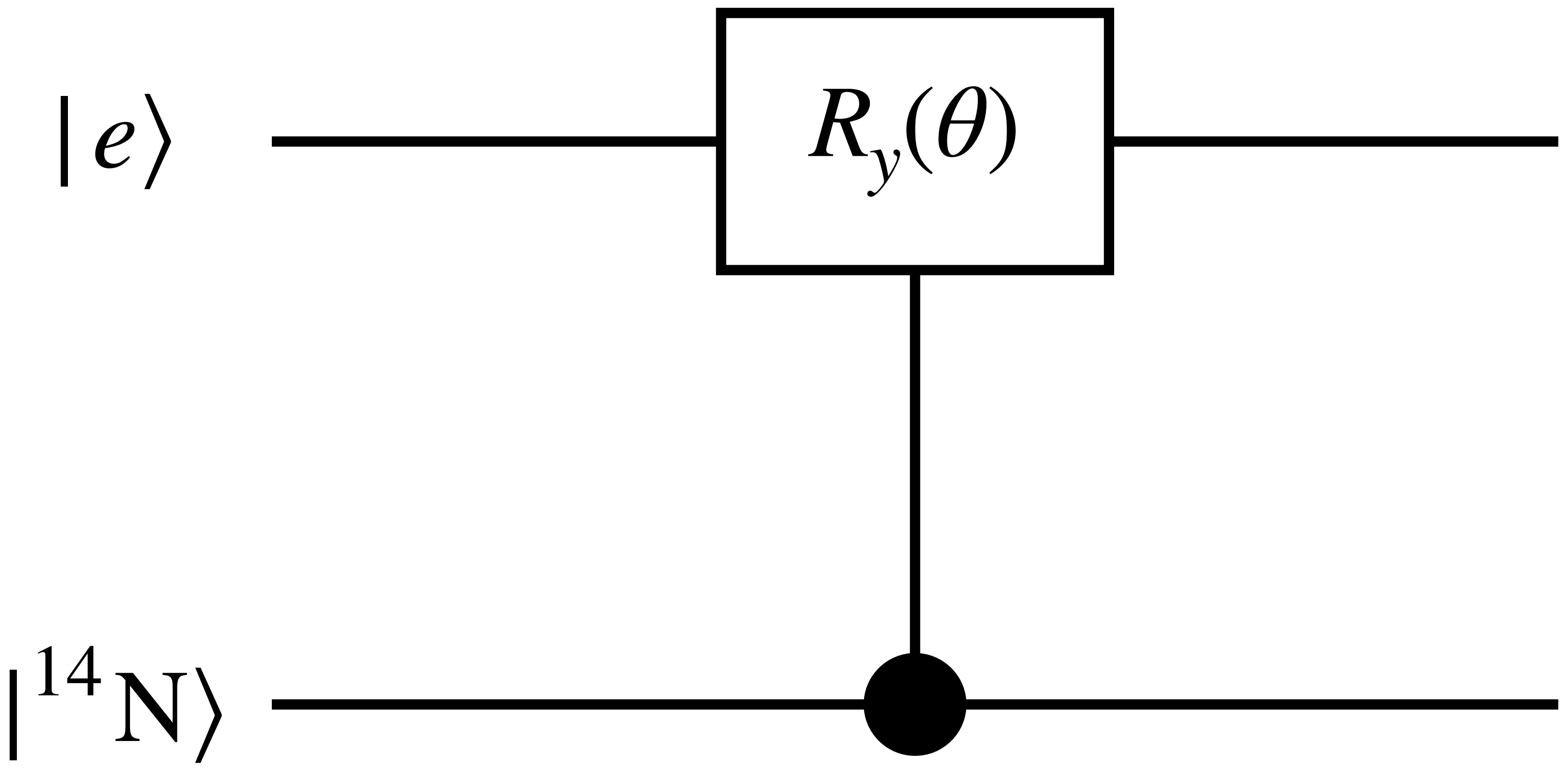

Manipulation of nuclear spins

- Mixing between e^- ($\vec{S}$) and $^{14}\mathrm{N}$ ($\vec{I}$) spin states caused by $H_{\mathrm{hyp}} = AS_zI_z$ allows the controlled-manipulation

Dutt+, Science (2007)
Neumann+, Nature (2010)
van der Sar+, Nature (2012)

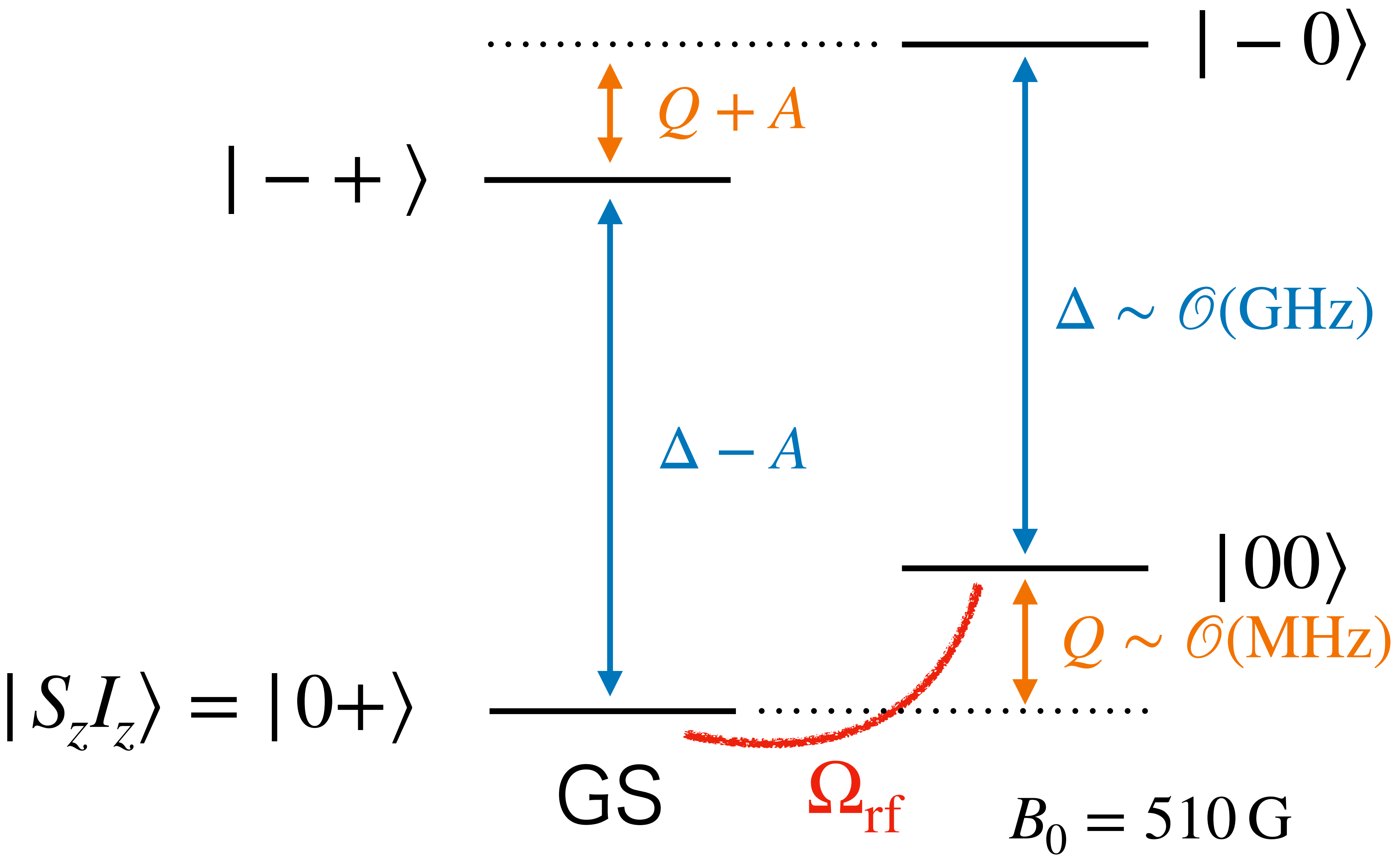

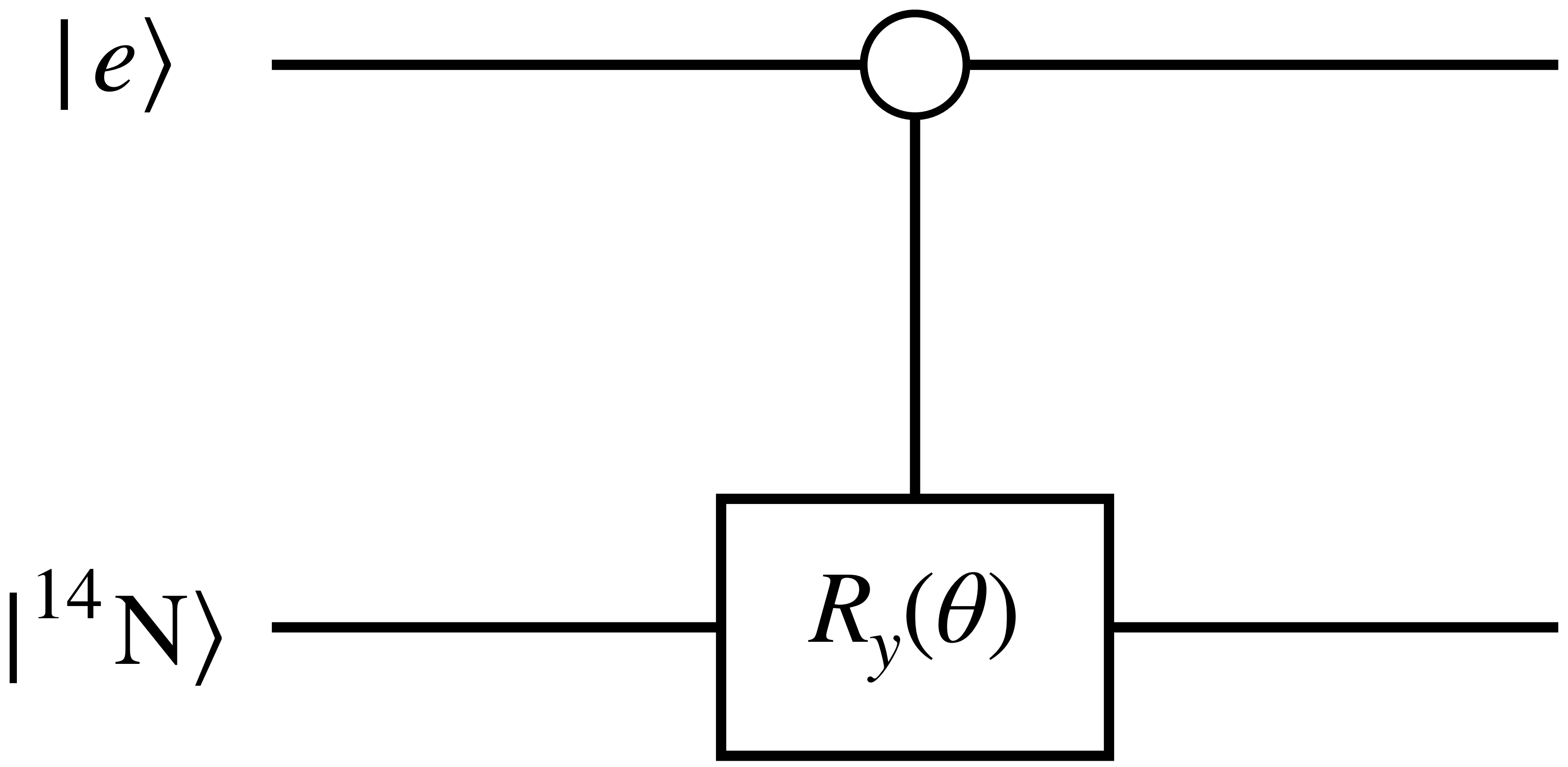

General manipulation & measurement

- Controlled-$R_x(\pi) \sim$ CNOT is the unique essential building block of general operation

- General $SU(4)$

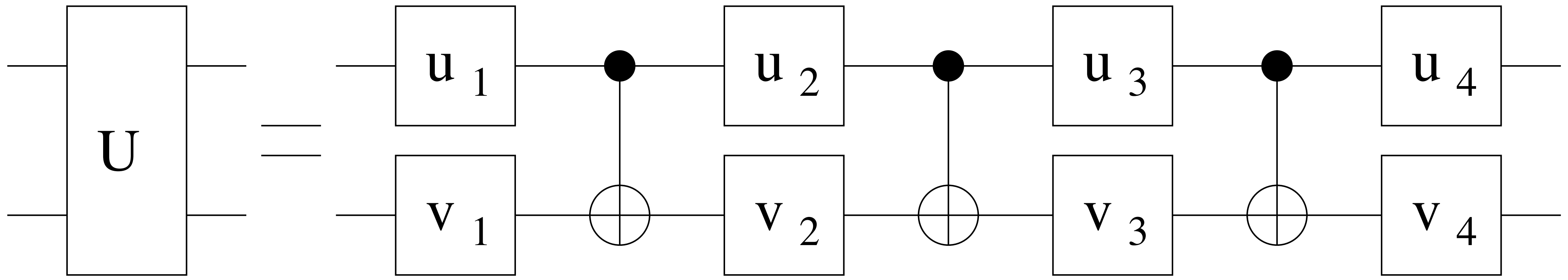

(# of CNOTs) ≤ 3

Vidal & Dawson, PRA (2003)

- Nuclear spin measurement

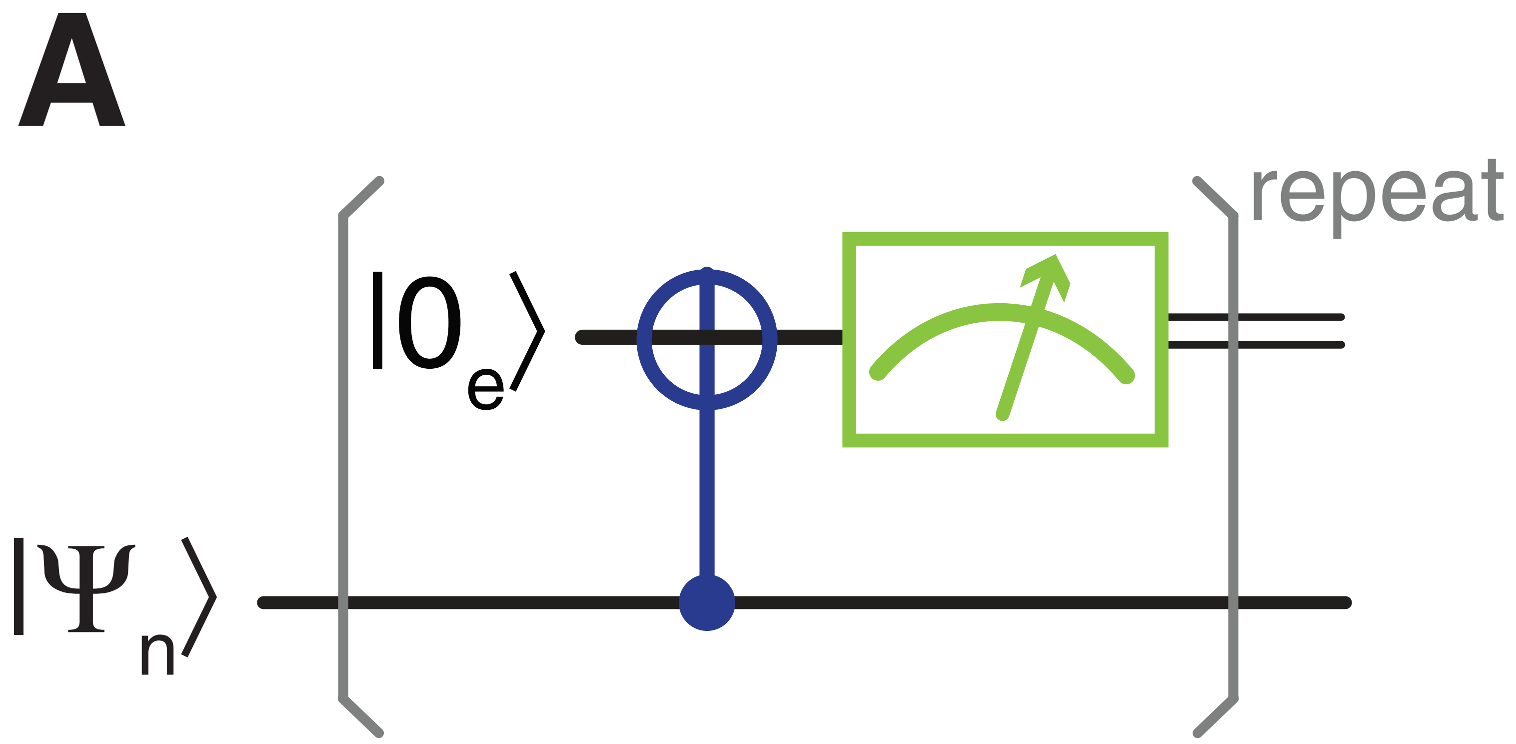

Neumann+, Nature (2010)

General manipulation & measurement

- Controlled-$R_x(\pi)$ ~ CNOT is the unique essential building block of general operation

- General $SU(4)$

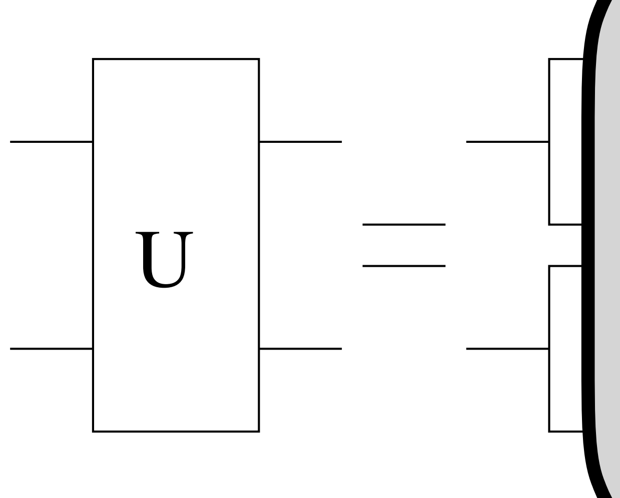

(# of CNOTs) ≤ 3

Vidal & Dawson, PRA (2003)

- Nuclear spin measurement

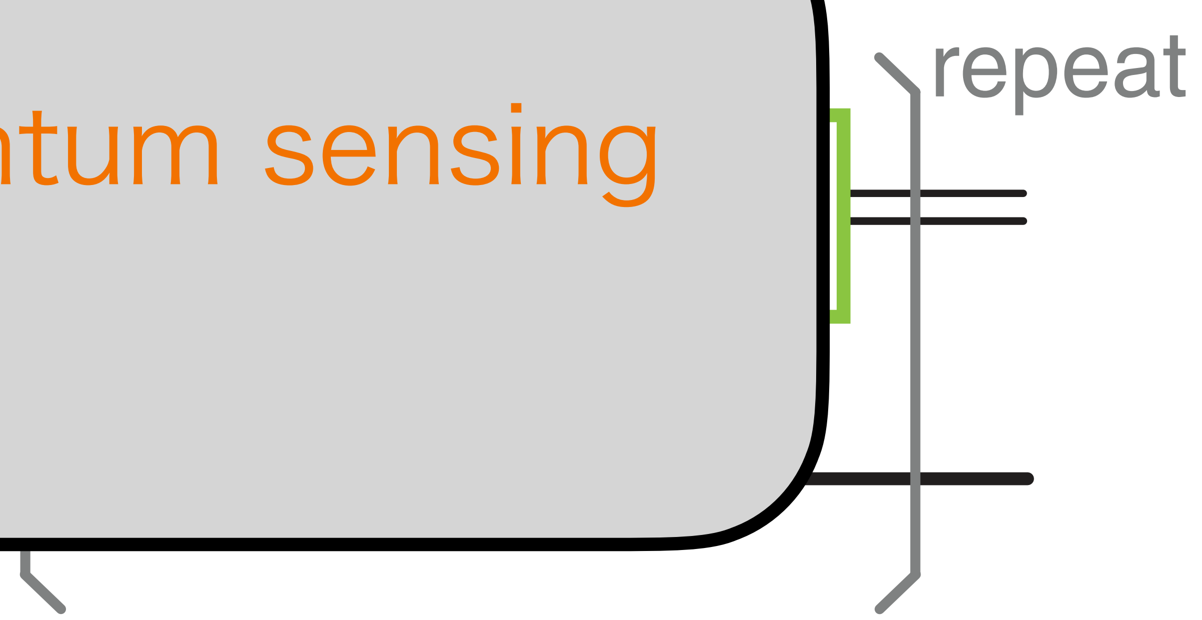

Nuclear spins of ^{14}N can be used for quantum sensing in the same way as electron spins!

Neumann+, Nature (2010)

Composition of $^{14}\mathrm{N}$ spin

- $^{14}\mathrm{N}$ is one of the rare stable odd-odd nuclei with spin $I = 1$
- Nuclear shell model description

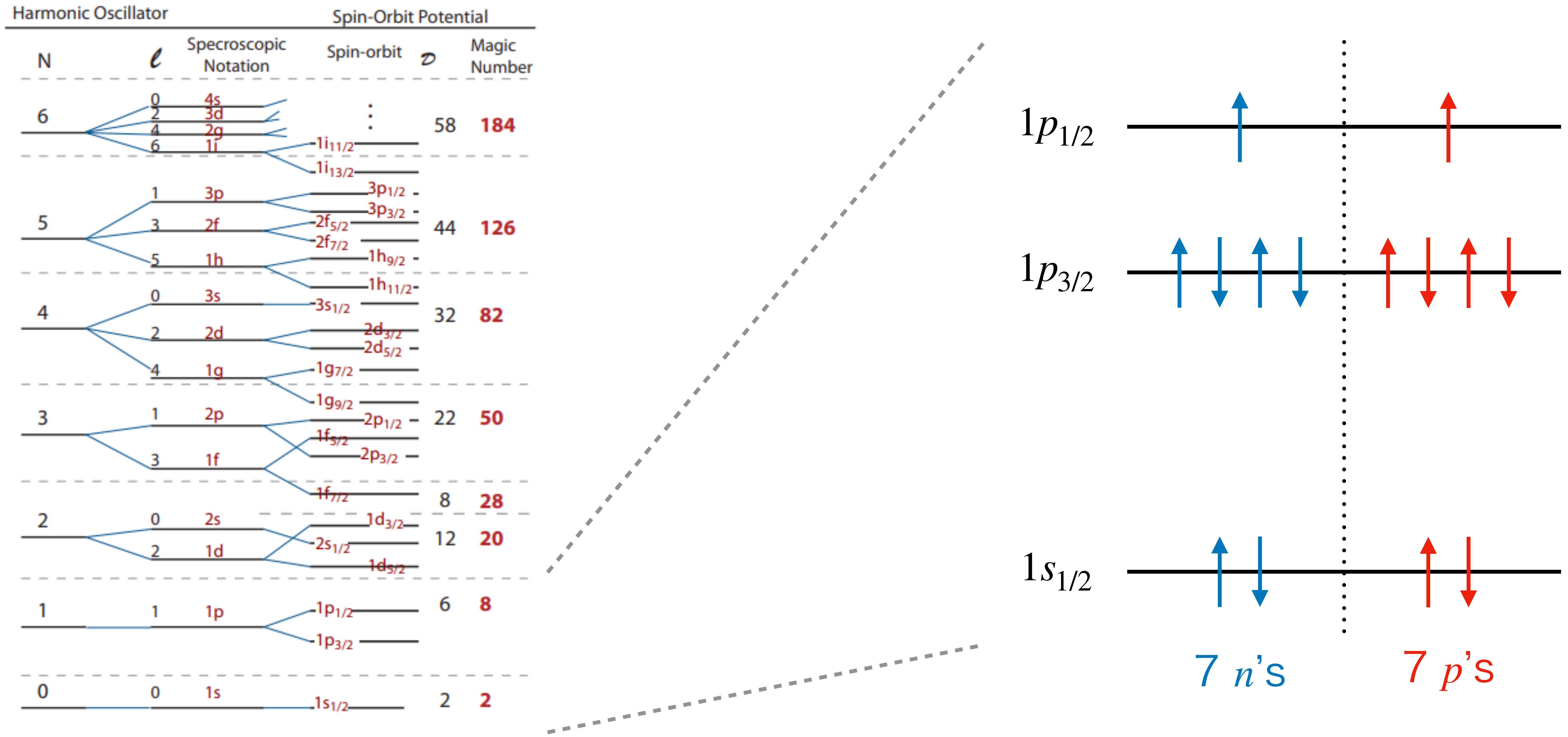

"Introductory Nuclear Physics" by K. S. Krane

Axion-$^{14}\mathrm{N}$ spin interaction

- A little algebra of spin synthesis

$$\left(2_{1/2}\otimes 3_1\right)\otimes\left(2_{1/2}\otimes 3_1\right)$$

Axion-$^{14}\mathrm{N}$ interaction

- A little algebra of spin synthesis

$$\left(2_{1/2} \otimes 3_1\right) \otimes \left(2_{1/2} \otimes 3_1\right)$$

$$= \left(\boxed{2_{1/2}} \oplus 4_{3/2}\right) \otimes \left(\boxed{2_{1/2}} \oplus 4_{3/2}\right)$$

Axion-$^{14}\mathrm{N}$ interaction

- A little algebra of spin synthesis

$$\left(2_{1/2} \otimes 3_1\right) \otimes \left(2_{1/2} \otimes 3_1\right)$$

$$= \left(\boxed{2_{1/2}} \oplus 4_{3/2}\right) \otimes \left(\boxed{2_{1/2}} \oplus 4_{3/2}\right)$$

$$= \left(1_0 \oplus \boxed{3_1}\right) \oplus \left(3_1 \oplus 5_2\right) \oplus \left(3_1 \oplus 5_2\right) \oplus \left(1_0 \oplus 3_1 \oplus 5_2 \oplus 7_3\right)$$

Axion-^{14}N interaction

- A little algebra of spin synthesis

$$(2_{1/2}\otimes 3_1)\otimes(2_{1/2}\otimes 3_1)$$

$$=(\boxed{2_{1/2}}\oplus 4_{3/2})\otimes(\boxed{2_{1/2}}\oplus 4_{3/2})$$

$$=(1_0\oplus\boxed{3_1})\oplus(3_1\oplus 5_2)\oplus(3_1\oplus 5_2)\oplus(1_0\oplus 3_1\oplus 5_2\oplus 7_3)$$

- $H_{\mathrm{int}}=\gamma_n\overrightarrow{B}^{(n)}_a\cdot\vec{S}_n+\gamma_p\overrightarrow{B}^{(p)}_a\cdot\vec{S}_p$

$$=\gamma_{^{14}\mathrm{N}}\overrightarrow{B}_a\cdot\vec{I}+\cdots$$

$$\left|\overrightarrow{B}_a\right|\propto\frac{1}{6}\left(\frac{g_{ann}}{m_n}+\frac{g_{app}}{m_p}\right)$$

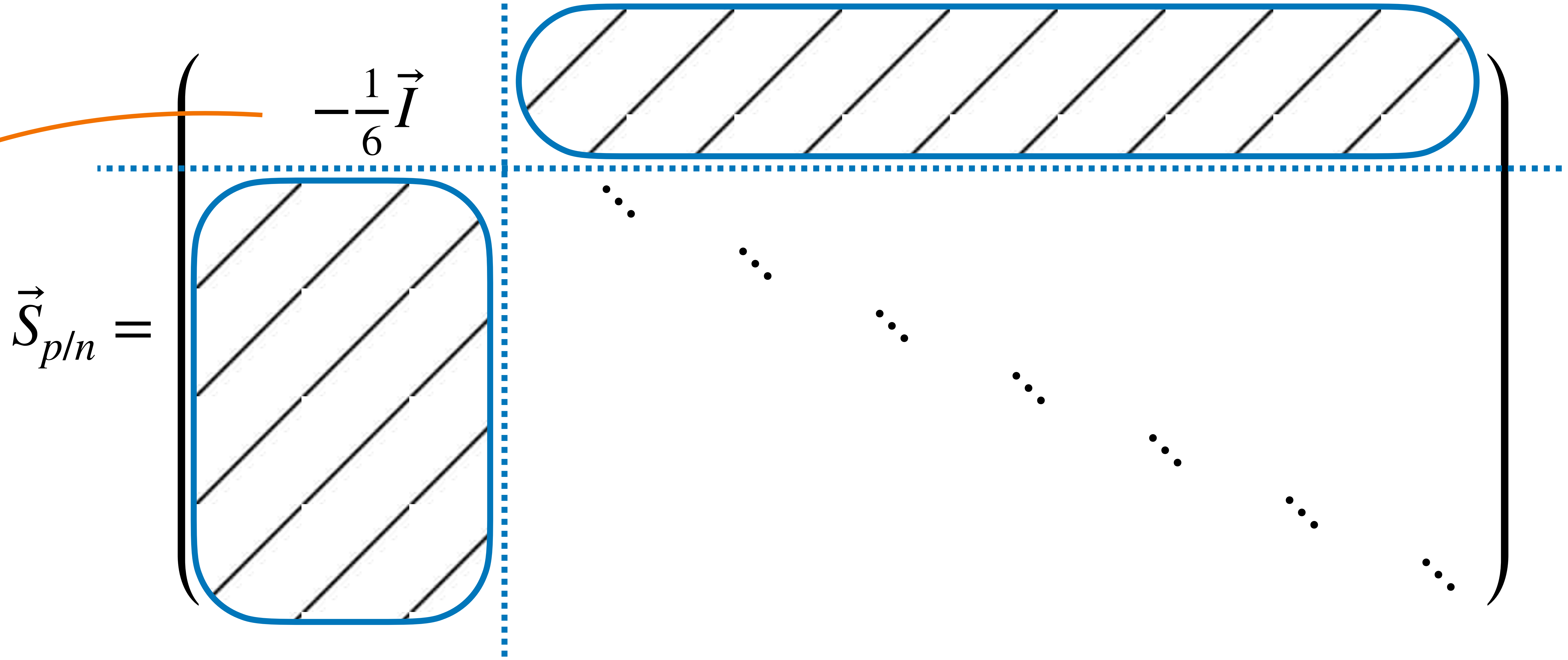

Constraints on axion-nucleon coupling

- Constraints on $\tilde{f}_a \equiv \left| \frac{g_{ann}}{2m_n} + \frac{g_{app}}{2m_p} \right|^{-1}$ with $\tilde{f}_a \sim \mathcal{O}(f_a)$ enhanced by long $T_{2n}^* \sim 7\,\mathrm{ms}$

Waldherr+, Nat. Nano. (2011)

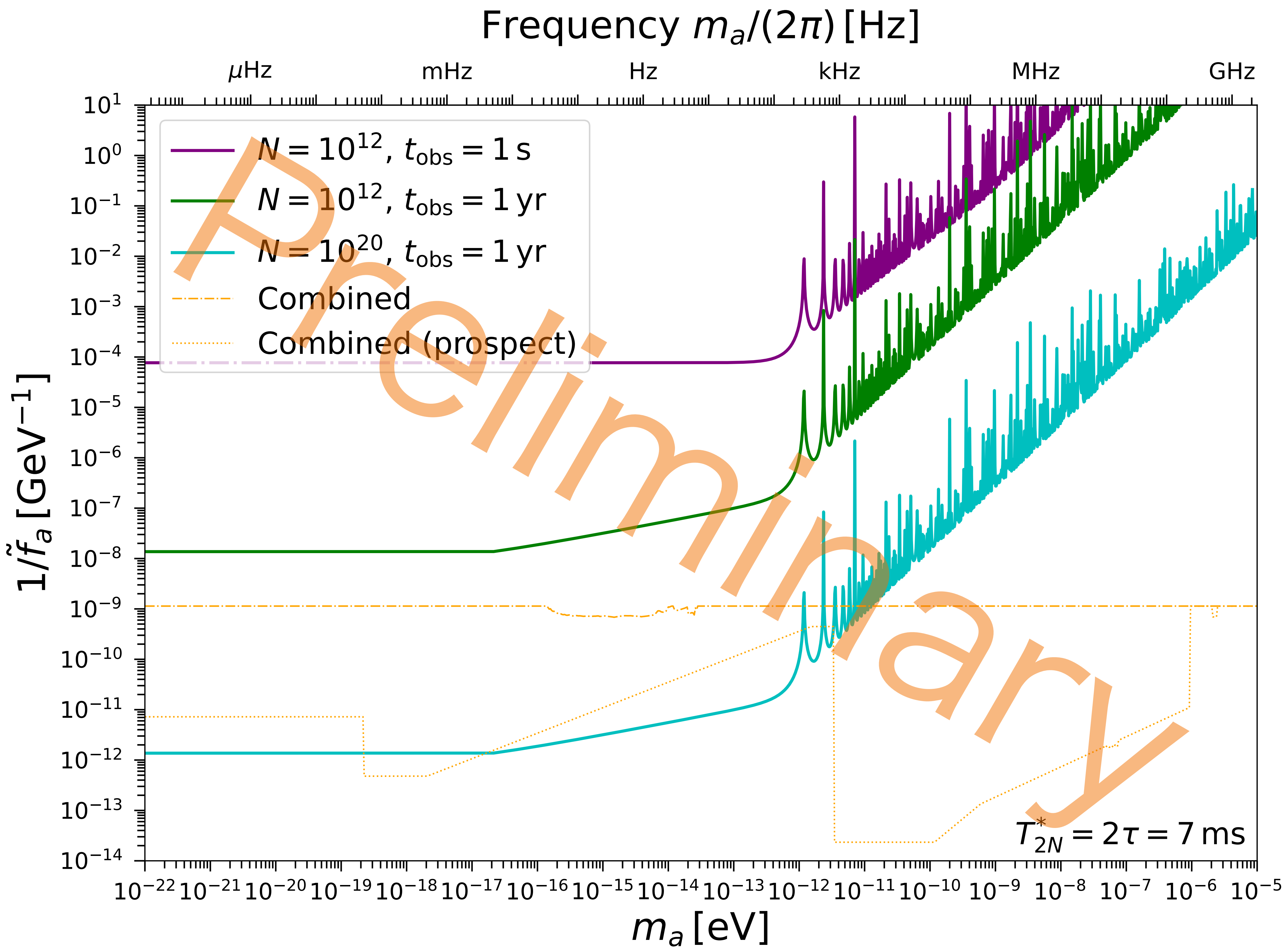

Comagnetometry

- Recap: constraints on axion couplings from K-$^3\mathrm{He}$ comagnetometer

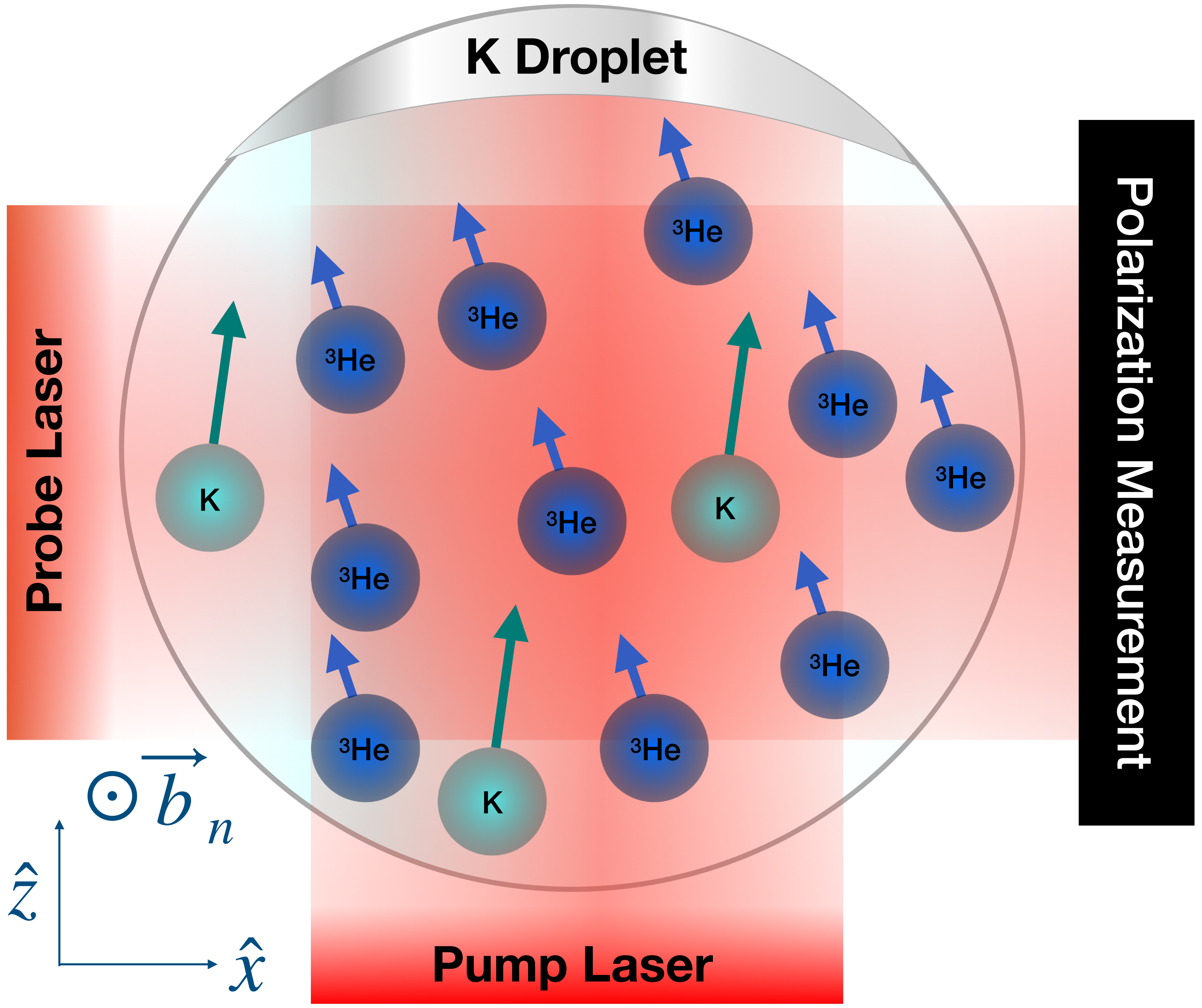

Bloch, Hochberg, Kuflik & Volansky
J. High Energ. Phys. (2020) 2020: 167

- At the compensation point $B_z = B_c$, insensitive to $\vec{B}_\perp$ but sensitive to $\vec{B}_{a,\perp}$

Protocol for “comagnetometry”

- A protocol to cancel out DC magnetic noise effects

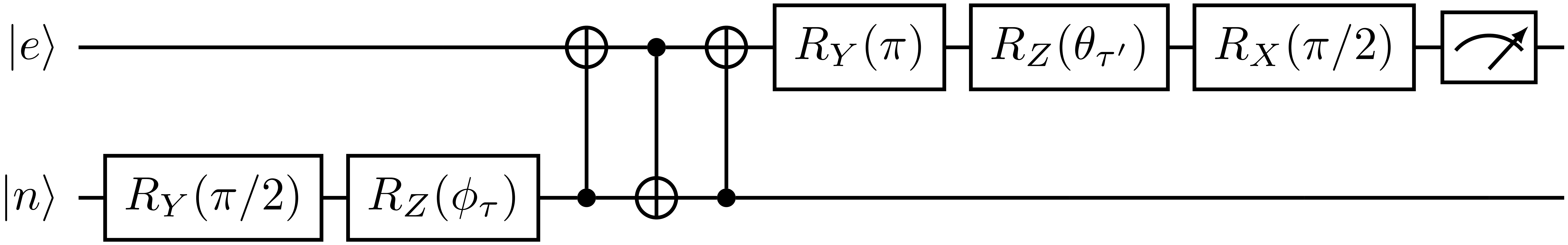

$$\frac{\text{magnetic field coupling with } e^-}{\text{magnetic field coupling with } {}^{14}\text{N}} = \frac{\gamma_e}{\gamma_N} \neq \frac{\text{axion coupling with } e^-}{\text{axion coupling with } {}^{14}\text{N}} = \frac{g_{aee}}{g_{aNN}}$$

- $\tau \sim T^*_{2N} \sim 1\,\text{ms},\ \tau' \sim T^*_{2e} \sim 1\,\mu\text{s},\ \frac{\tau}{\tau'} = \frac{\gamma_e}{\gamma_N}$ works well!

Discussions and conclusions

- We explored the potential of NV center magnetometry for DM search

- Benefits of this approach include:
  - Wide dynamic range = broad DM mass coverage
  - Sensitivity to electron, neutron, and proton spins

- Some applications of advanced quantum metrology techniques
  - Entanglement
  - Comagnetometry protocol
  - Ancilla-assisted frequency upconversion

International Center for
Quantum-field Measurement Systems for
Studies of the Universe and Particles
WPI research center at KEK

- Now setting up an experimental environment at QUP with NV + cryogenic

Backup slides

Axion DM parameter space

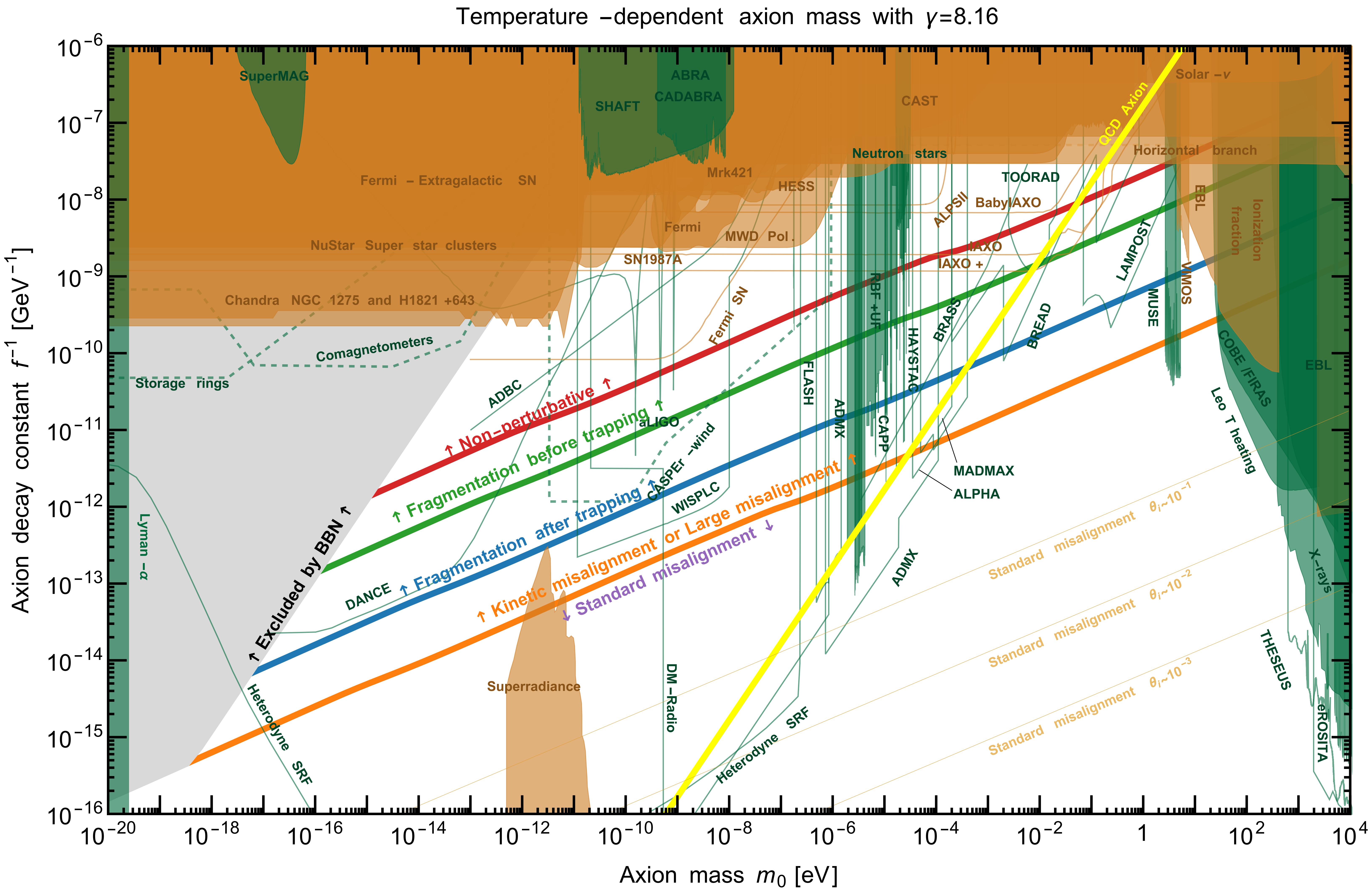

Eröncel+ [2206.14259]

Sensitivity estimation

- The outcome of the spin-projection noise

$$|x\rangle \equiv \frac{1}{\sqrt{2}}\left(|0\rangle + |+\rangle\right)$$

$$\Delta S \equiv \frac{1}{2}\left[\langle x|\sigma_z^2|x\rangle - \left(\langle x|\sigma_z|x\rangle\right)^2\right]^{1/2} = \frac{1}{2}$$

- Noise contribution is $\Delta S_{\mathrm{sp}} \sim \begin{cases} \frac{1}{2}\frac{1}{\sqrt{N(t_{\mathrm{obs}}/\tau)}} & (t_{\mathrm{obs}} < \tau_a) \\ \frac{1}{2}\frac{1}{\sqrt{N(\tau_a/\tau)}}\frac{1}{\left(t_{\mathrm{obs}}/\tau_a\right)^{1/4}} & (t_{\mathrm{obs}} > \tau_a) \end{cases}$

- Sensitivity curve is $(\mathrm{SNR}) \equiv \frac{S}{\Delta S_{\mathrm{sp}}} = 1$

Sensitivity estimation

- The axion-induced effective magnetic field has an unknown velocity $\mathbf{v}_{\mathrm{DM}}$ and phase δ

$$\mathbf{B}_{\mathrm{DM}} \simeq \sqrt{2\rho_{\mathrm{DM}}}\frac{g_{aee}}{e}\mathbf{v}_{\mathrm{DM}}\sin(m_{\mathrm{DM}}t+\delta)$$

Random velocity $\mathbf{v}_{\mathrm{DM}}$

- The signal is proportional to $\left(v_{\mathrm{DM}}^i\right)^2$ $(i=x,y,z)$, which is averaged to $\sim \frac{1}{3}v_{\mathrm{DM}}^2$

Random phase $\delta \in [0,2\pi)$

- The signal is estimated as a function of δ : $S(\delta) \propto \cos\left(\frac{m\tau}{2}+\delta\right)$

- We obtain the average $\langle S\rangle_\delta = 0$ and the standard deviation $\sqrt{\langle S^2\rangle} \neq 0$, which should be compared with the noise

Technical noise mitigation

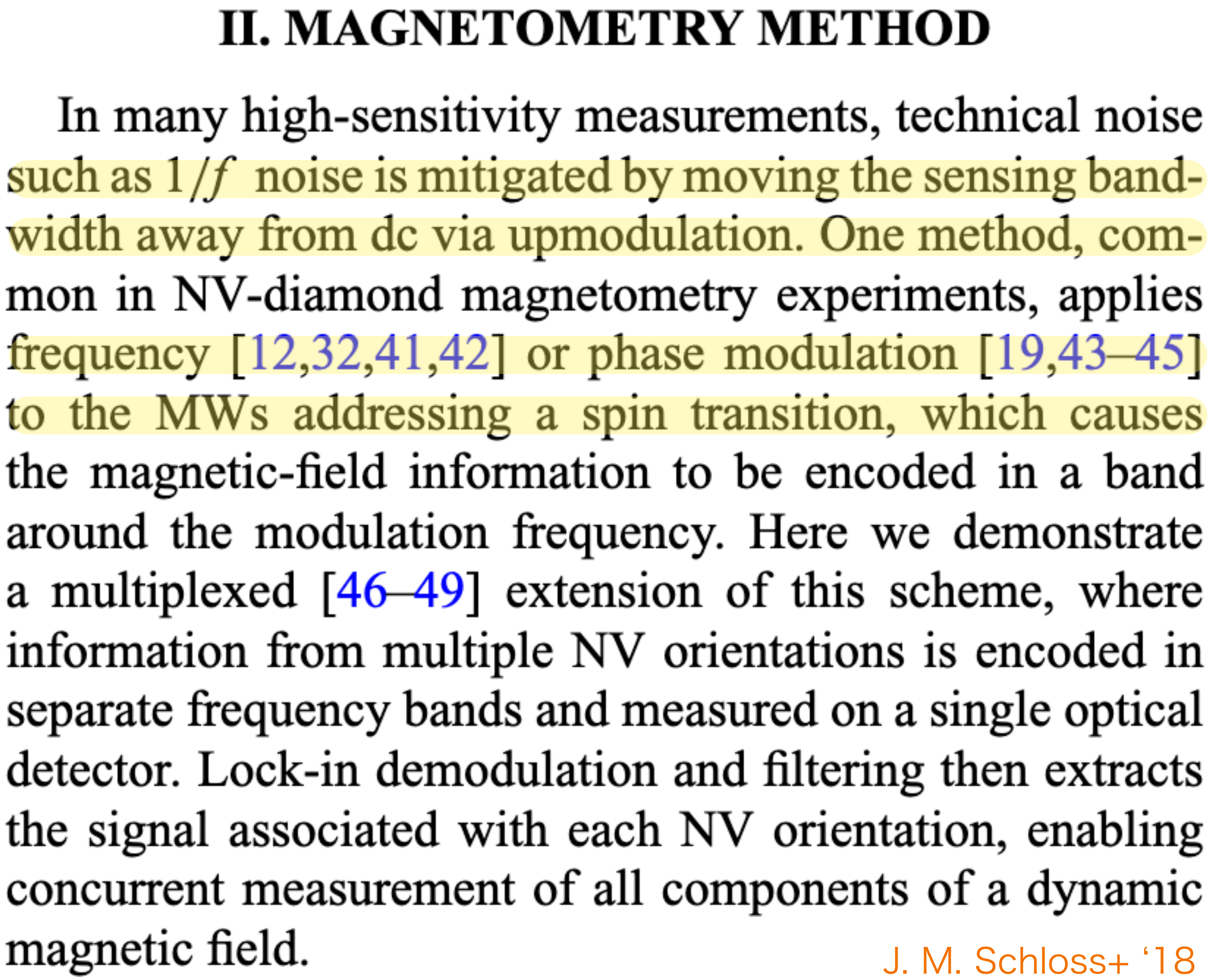

II. MAGNETOMETRY METHOD

In many high-sensitivity measurements, technical noise such as $1/f$ noise is mitigated by moving the sensing bandwidth away from dc via upmodulation. One method, common in NV-diamond magnetometry experiments, applies frequency [12,32,41,42] or phase modulation [19,43–45] to the MWs addressing a spin transition, which causes the magnetic-field information to be encoded in a band around the modulation frequency. Here we demonstrate a multiplexed [46–49] extension of this scheme, where information from multiple NV orientations is encoded in separate frequency bands and measured on a single optical detector. Lock-in demodulation and filtering then extracts the signal associated with each NV orientation, enabling concurrent measurement of all components of a dynamic magnetic field.

J. M. Schloss+ ‘18

Comparison among different T_n^*

- $T_2^* \sim 7\,\mathrm{ms}$ is observed, many attempts to make it longer in literature

Waldherr+, Nat. Nano. (2011)

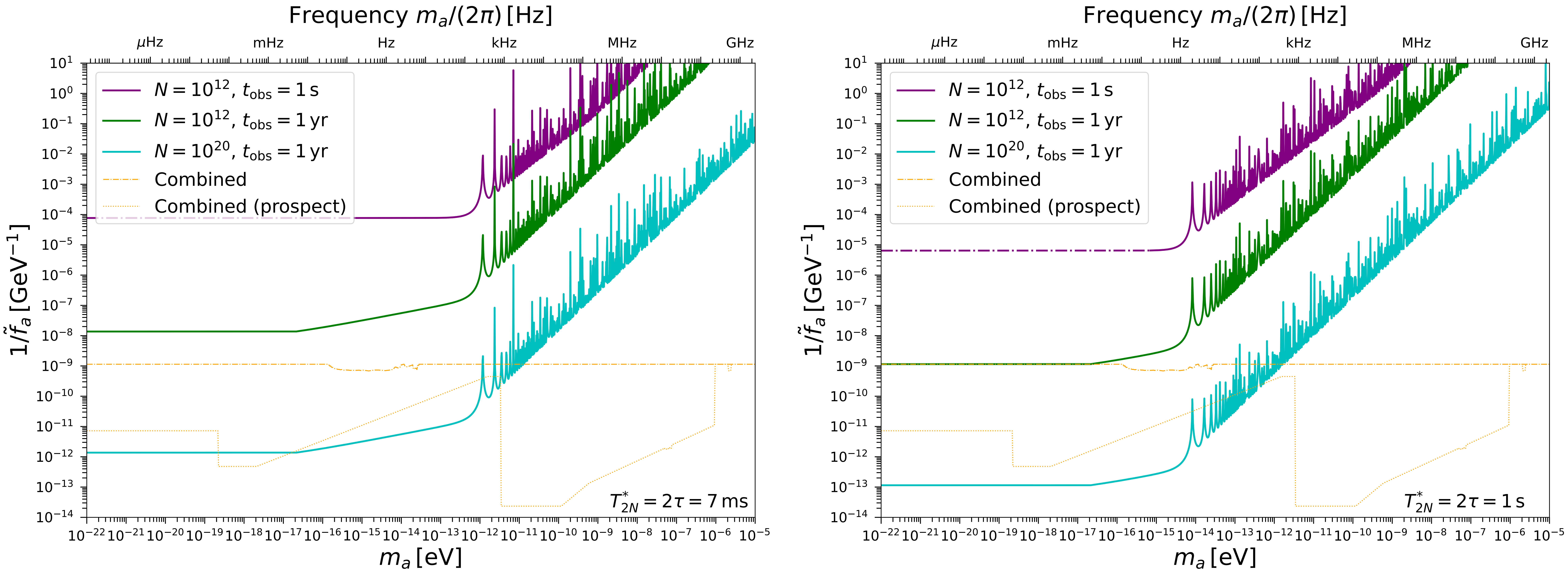

Constraints on g_{ann} and g_{app}

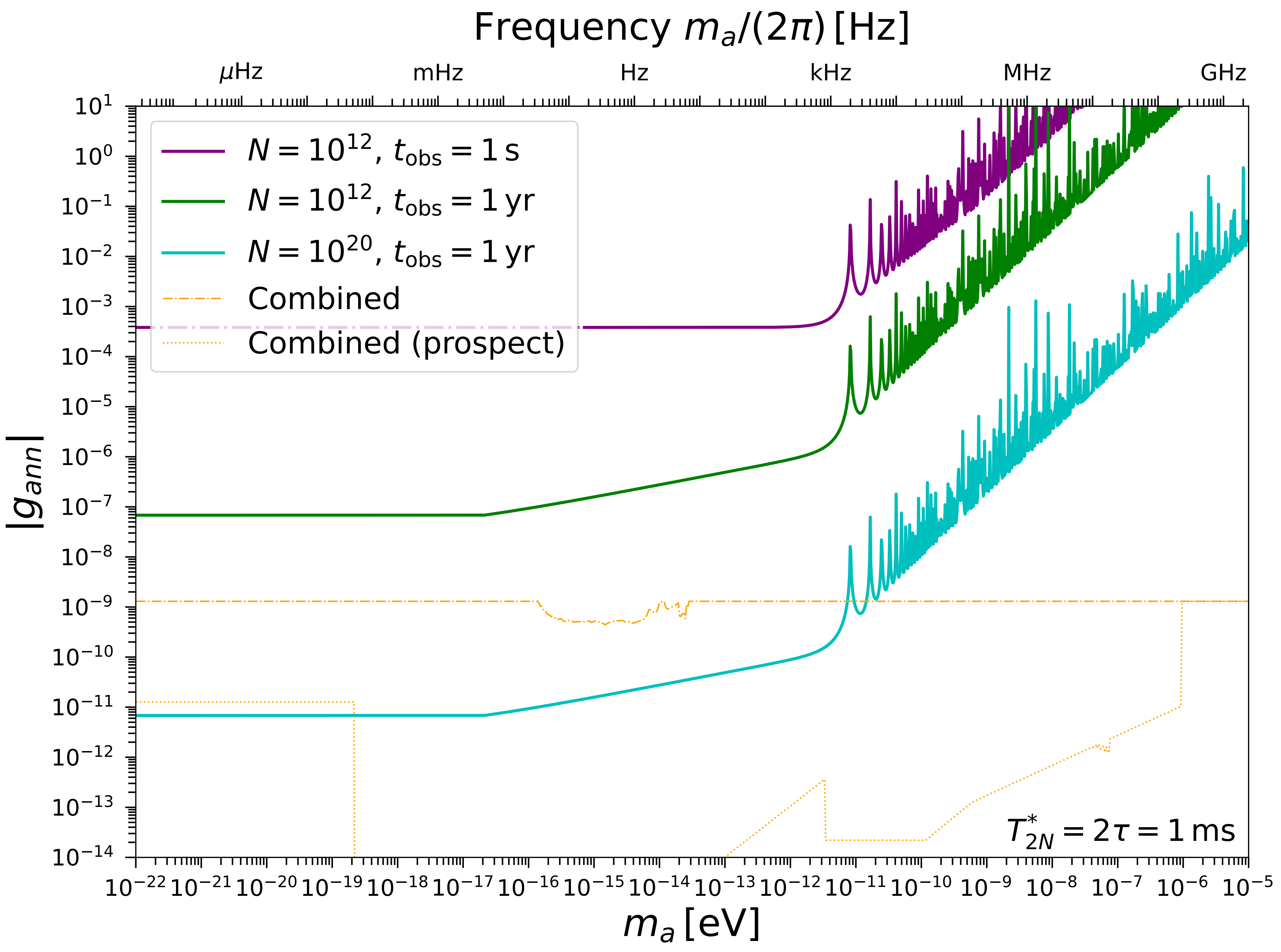

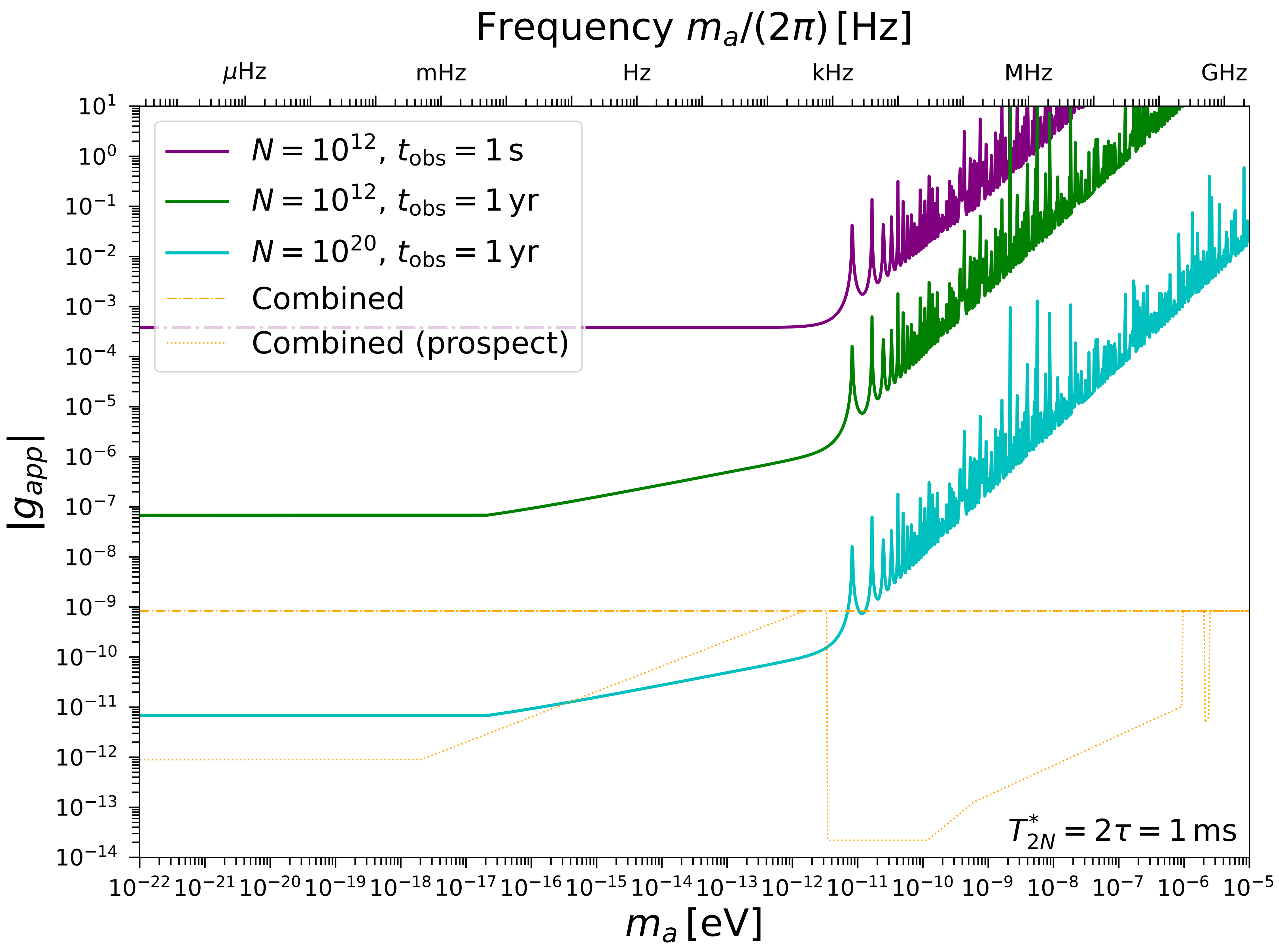

Hahn-echo sequence of ^{14}N spins

- $T_2 \sim 9\,\mathrm{ms}$ is observed Aslam, et al. ‘17

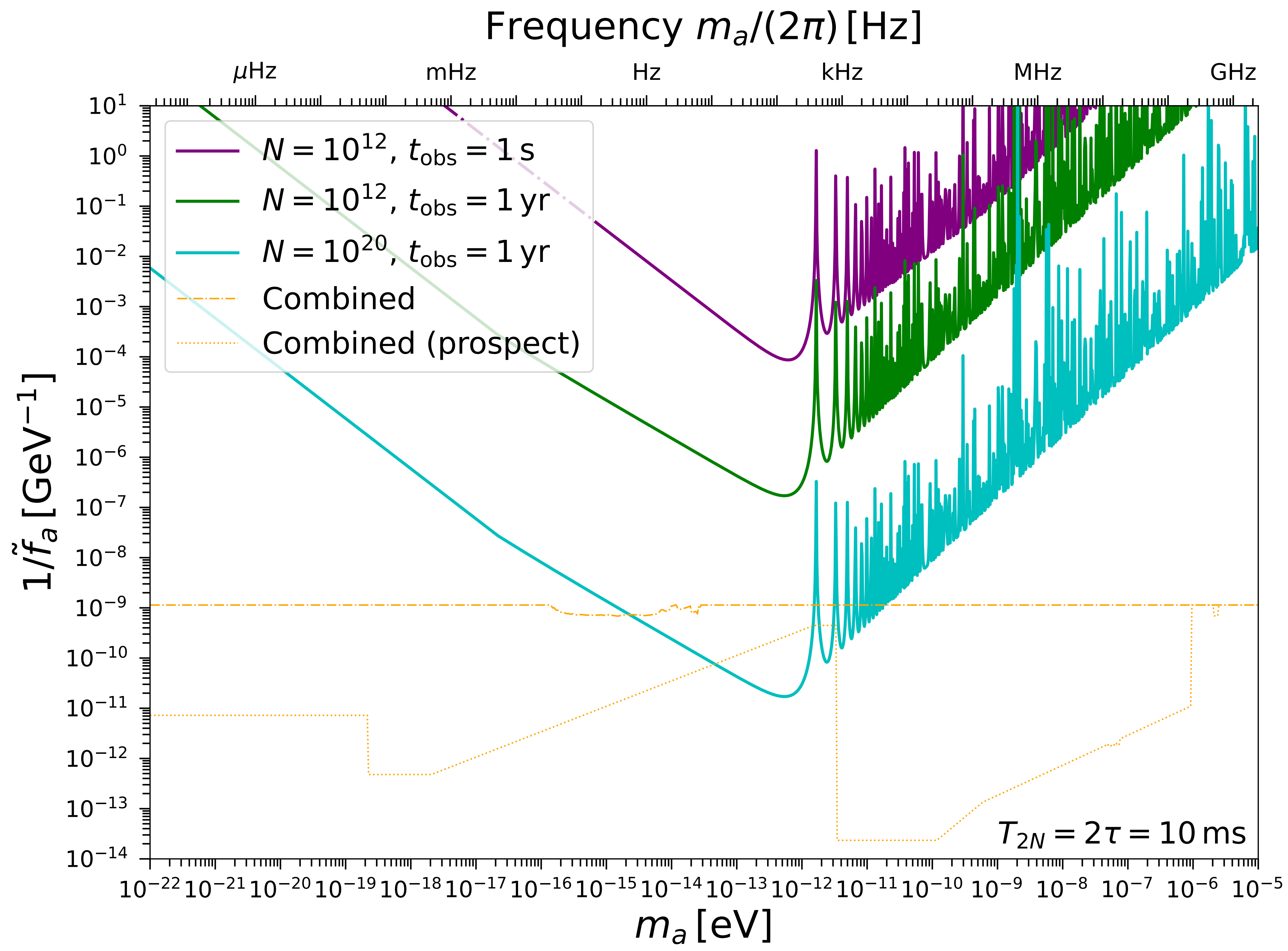

Plan of QUP quantum sensor cluster

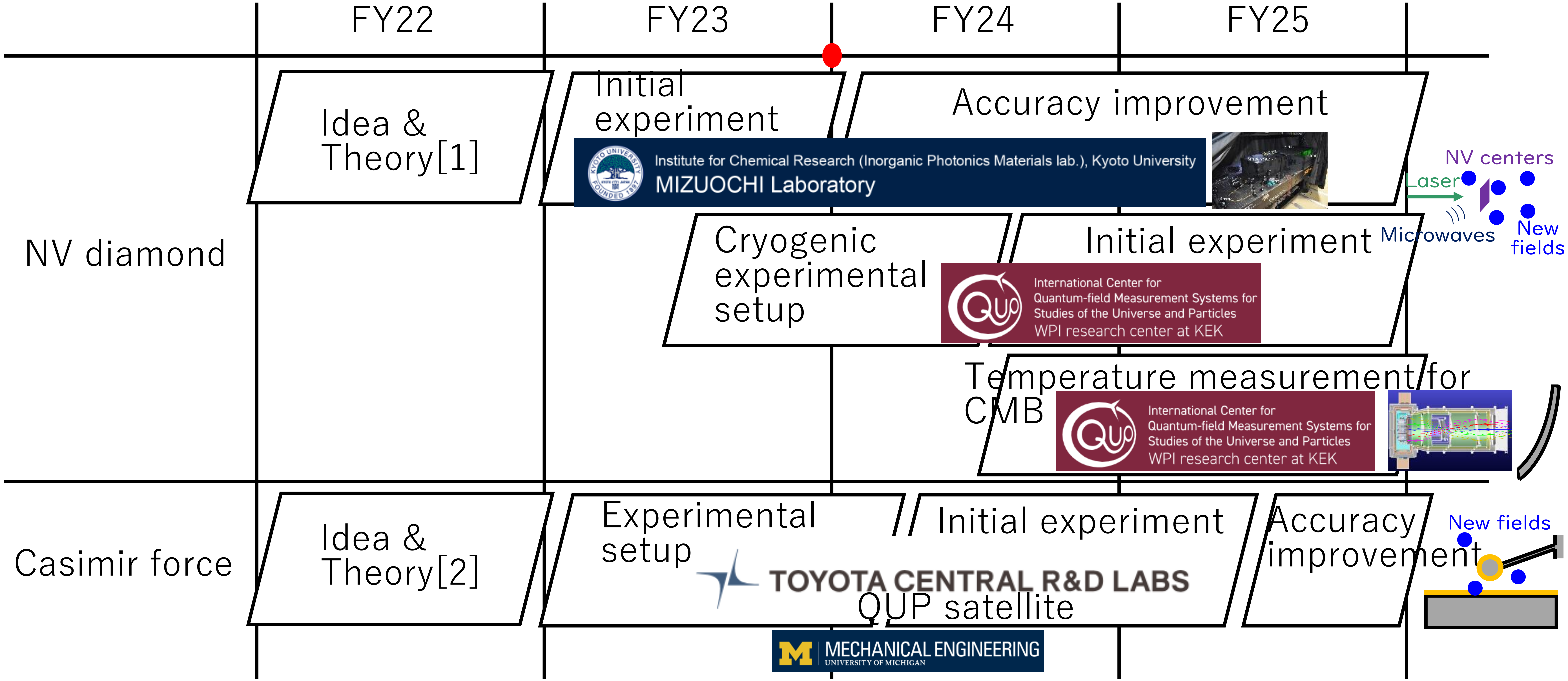

FY22 FY23 FY24 FY25

NV diamond

Idea & Theory[1]

Initial experiment

Institute for Chemical Research (Inorganic Photonics Materials lab.), Kyoto University
MIZUOCHI Laboratory

Accuracy improvement

Cryogenic experimental setup

Initial experiment

International Center for Quantum-field Measurement Systems for Studies of the Universe and Particles
WPI research center at KEK

Temperature measurement for CMB

International Center for Quantum-field Measurement Systems for Studies of the Universe and Particles
WPI research center at KEK

Casimir force

Idea & Theory[2]

Experimental setup

TOYOTA CENTRAL R&D LABS

Initial experiment

QUP satellite

MECHANICAL ENGINEERING
UNIVERSITY OF MICHIGAN

Accuracy improvement

[1] S. Chigusa, M Hazumi, E. D. Herbschleb, N. Mizuochi, and K. Nakayama, “Light dark matter search with nitrogen-vacancy centers in diamonds,” arXiv:2302.12756.
[2] Y. Ema, M. Hazumi, H. Iizuka, K. Mukaida, and K. Nakayama, “Zero Casimir force in axion electrodynamics and the search for a new force,” Physical Review D 108, 016009 (2023).

Credit: H. Iizuka @ QUP week 2024